FINITE ELEMENT ANALYSIS OF BIO-HEAT TRANSFER FOR MAGNETIC FLUID HYPERTHERMIA APPLICATION

by

KAMALKUMAR N CHAUHAN

Presented to the Faculty of the Graduate School of
The University of Texas at Arlington in Partial Fulfillment
of the Requirements
for the Degree of

MASTER OF SCIENCE IN MECHANICAL ENGINEERING

THE UNIVERSITY OF TEXAS AT ARLINGTON

December 2009

ACKNOWLEDGEMENTS

I would like to thank my supervising professor Dr. Brian Dennis for his continuous guidance and encouragement thorough my thesis work. I was very lucky to work under him as his teaching assistant. I would also like to express my gratitude towards Dr. Kent Lawrance and Dr. Zhen Xue Han for being on my committee.

I am especially grateful to Harsh Shah and Dr. Rajeev Kumar for their help during my thesis work. I would also like to extend my thanks the following at CFD lab: Monal, Darshak, Lha, Katie, Ai and Chinmay for their friendship and co-operation.

Finally I would like to express my deep gratitude towards my elder sister Aarti who has been encouraging and inspiring me to pursue graduate studies. I would like to thank my parents for supporting me and always encouraging me for this great opportunity of education. I am also thankful to my nephew Sarvesh and my younger brother Hitesh for being supportive. I would also like to thank all my friends who have helped me throughout my career

November 6, 2009

ABSTRACT

FINITE ELEMENT ANALYSIS OF BIO-HEAT TRANSFER

FOR MAGNETIC FLUID HYPERTHERMIA

APPLICATION

Kamalkumar N Chauhan, M.S

The University of Texas at Arlington, 2009

Supervising Professor: Brian H. Dennis

Finite Element solution for the multi-region bio-heat Equation is present to model magnetic fluid hyperthermia. This study solves the Penne's two dimensional bio-heat equation using finite element method and develops the thermal behavior of the tumor and healthyportion of the composite tissue using low curie nanoparticles.

The inner cylinder represents the tumor tissue containing low Curie temperature nanoparticles. Low Curie temperature nanoparticles generate heat due to the Neel and Brownian relaxation when a magnetic field is applied. The outer cylinder represents the healthy tissue.

First part of this thesis discusses about the background related to the nanoparticles heat dissipation and finite element procedure. Second part of thesis deals with the computer implementation of the finite element method. Last part discusses the numerical results of this thesis.

Numerical results indicate that tumor region is heated without adversely affecting too much of the healthy region. Optimized distribution of the low curie nanoparticles in the tumor tissue can significantly control the temperature in tumor region in hyperthermia therapy.Different boundary conditions and different blood perfusion rates, irregular geometry have been taken into consideration in this thesis.

TABLE OF CONTENTS

LIST OF ILLUSTRATIONS

LIST OF TABLES

CHAPTER 1

MAGNETIC FLUID HYPERTHERMIA (MFH)

1.1 Introduction

When Pennes developed the bio-heat equation with heat transfer and blood perfusion term, many researchers tried to solve it for different applications, both numerically and analytically. In recent decades, this Pennes' equation has been used to model hyperthermia cancer therapy. Hyperthermia cancer treatment has proven to be an effective method in cancer treatment compare to surgery, chemotherapy and radiation. In Hyperthemia cancer treatment involves heating a tumor region to 43℃ to 45℃ [1]. Even though this temperature is unpleasant for the patient, cancer cells are more susceptible to this temperature range and can be killed over a period of time. These methods cause minimal damage to the healthy tissue therefore leaving limited negative side effects in this treatment. Sometimes oncologists often use hyperthermia cancer treatment in combination with radiotherapy and chemotherapy. In addition to the eliminating many cancer cells, hyperthermia can make resistant cells more vulnerable to other treatment.

Hyperthermia can treat for specific location or the entire body. Local hyperthermia applied externally to tumor region near the skin surface. Hyperthermia focuses microwave laser or ultrasonic energy on disease tissue for larger tumor or multiple tumor location.

1.2 Magnetic fluid hyperthermia cancer treatment

Gilchrist and other proposed the use of magnetic material in hyperthermia in 1957 [1]. Magnetic particles exhibit ferro or ferromagnetic properties. This particle display magnetism even in the absence of an applied magnetic field. Magnetic particles that use in hyperthermia cancer have permanent magnetic orientation or moment. Applied alternate magnetic field provides the necessary energy to magnetic particles to reorient the particles

magnetic moment. This magnetic energy when dissipated is converted to thermal energy. In addition, change in the magnetic moments can force the nanoparticles to physically rotate. Hyperthermia cancer treatment uses this thermal energy to destroy the cancer cells effectively. As nanoparticles rotate through viscous fluid to return to their equilibrium position, heat also has been generated this time. However this heat contributes very little in total heat generation.

Pankhurst and others have also described the heating in nanoparticles[1]. Particles with diameter 10 nanometers demonstrate super magnetic properties. The magnetic moment of super magnetic nanoparticles is randomly oriented by the thermal energy and they do not produce magnetism in the absence of the magnetic field. Unlike ferro and ferromagnetic materials, they do not aggregate after exposure to the magnetic field. Aggregation can hinder the body's effort to remove the nanoparticles. Therefore super magnetic nanoparticles are ideal candidates for the hyperthermia cancer treatment.

Magnetic fluids are generally made of magnetic nanoparticles dispersed in water or hydrocarbon fluid. Here we use magnetic fluids for medical applications so we need to check both compatibility of fluid and nanoparticles. Also fluid should have neutral pH value and physiological salinity. Nanoparticles should be distributed evenly throughout the magnetic fluid and also nanoparticles should be small enough so that precipitation can be avoided because of the gravitational force. Magnetic material should not be toxic. Generally Fe_3O_4 is a common choice to use as a magnetic nanoparticle. Magnetic nanoparticles should be uniform in size and shape.

Synthesis methods generate the nanoparticles in uniform size and shape. Two most common techniques include solution chemistry and aerosol/vapor are used in synthesis methods. In solution chemistry, homogeneous reactions are used to prepare nanoparticles. This reaction occurs in two stages: particle formation and growth. In particle formation, single group of particles form when solution reaches the critical saturation point. After that as solution adhere

to their surface, growth of the nanoparticle occurs. During growth stage, formation of the new nanoparticles should be avoided.

Aerosol/vapor method use spray pyrolysis and laser pyrolysis[1]. Spray pyrolysis starts with aerosol droplet generator. This aerosol droplet generator produces fine droplets solution. This fine droplets solution pass through series reactor that evaporate the solvent and pyrolize the resulting nanoparticles. Laser pyrolysis technique employs continuous carbon dioxide laser to start nanoparticles formation reaction. Particle aggregation can be almost eliminated in laser pyrolysis and produce narrower particle size distribution. Both of this method produces large quantities of nanoparticles that are used in hyperthermia cancer treatment.

Once magnetic nanoparticles have been synthesized, magnetic fluid has been delivered to the tumor tissue. Several methods can be used to deliver the magnetic fluid in hyperthermia treatment. Magnetic fluid can be injected directly to the tumor tissue. Sometimes magnetic fluid can be injected to the artery which mixes with blood and supplies to the disease tissue. Group of small tumors whose location cannot be pinpointed uses different technique to inject magnetic fluid. Once the magnetic fluid delivers to the tumor region which includes magnetic nanoparticles, it produces localize heating in the tumor region, supplied antibodies to the magnetic nanoparticles via invascular injection make hyperthermia treatment more selective.

1.3 Low – Curie temperature naoparticles

Recently, researchers have quantitatively studied the MFH. The heating effect of embedded nanoparticles when applied to external magnetic field based on three dimensional bio-heat equations with space dependent thermo-physiological parameter indicates that nanoparticles produces high heating on target tissue, which is heavily dependent on magnetic properties of nanoparticles. *Xu et al*. [2] stimulated the temperature distribution in hyperthermia by an external ferrite core applicator in composite model and got an agreement between theoretical and experimental values. Because most of the nanoparticles under current

investigation have high Curie temperature, they produce temperature in tumor region well beyond the effective temperature of the hyperthermia.

The Curie temperature which is defined as the temperature where material loses its magnetic momentum and heating function is based on Neel relaxation which can be altered through material composition and size of the nanoparticles.

Although a high temperature is desired in tumor region but if temperature passes beyond the effective hyperthermia temperature, there is a significant damage in the healthy tissue. We can overcome this problem by selecting “self regulating” nanoparticles. By designing the low curie nanoparticles, temperature can be easily regulated. Nanoparticles with Curie temperature near the therapeutic hyperthermia range can effectively maintain the temperature between 42 ℃ - 47℃. These self regulating nanoparticles ensure disease tissues reach the necessary temperatures and at the same time it prevents the excessive heating in the healthy tissue thereby preventing damage in the healthy tissue.

CHAPTER 2

HEATING MAGNETIC FLUID WITH ALTERNATING MAGNETIC FIELD

2.1 Introduction

Magnetic nanoparticles are used for local hyperthermia, thermo ablative cancer therapy. Rosenweig's theory predicts that radio frequency magnetic heating of the ferrofluid depends on the size of the nanoparticles which is determined by magnetic moment, magnetic anisotropy and the viscosity of the fluid. Here material parameter of magnetic particles are strongly time dependent, heating rates are peak at certain temperature. Materials with low Curie temperature for which magnetic properties are strongly time dependent can explain the problem of self regulated heating of ferro-fluids.

Magnetic particles have been used in different biomedical applications from long decades. Magnetic nanoparticles are used as heat source in the presence of radio frequency for hyperthermia cancer treatment. By use of magnetic nanoparticle, tumor tissue can be heated in the range of 42-46 °C [3] in hyperthermia cancer treatment without much harm to the healthy surrounding tissue. Cancer cells are more susceptible in the temperature range of 42-46 °C. Tolerance limit of inductive heating of tissue limits the safe range of magnetic fluid amplitudes and frequency that can be applied to magnetic hyperthermia treatment. It has been shown that combination of magnetic field strength (H) and frequency (f) is biologically invasive when H*f is less than or equal to 4.85×10^8 Hz .A /m

During magnetic hyperthermia treatment, nanoparticles dissipate energy through eddy currents, hysteresis resonance and relaxation losses. This loss mechanism depends on the crystal perfection and micro magnetic switching of the nanoparticles. In magnetic fluid hyperthermia cancer treatment, we consider only hysteresis losses. These losses diminish near the curie temperature of the ferromagnetic material. If the composition of the

material is tuned so that Curie temperature is brought near the maximum temperature, heating can be self regulated so that tissue will not overheat. The heating rate also strongly depends on the saturation magnetization, Magnetic Anisotropy and carrier viscosity. In this thesis, we consider material properties of ferro-fluid with Curie temperature 42 °C - 47 °C which could be of interest in magnetic hyperthermia therapy application.

2.2 Power dissipation

From the first law of the thermodynamics

$$dU = \delta Q + \delta W \tag{2.1}$$

Where U is the internal energy and W is the magnetic work done on the system. Magnetic work in general is given by $\delta W = \vec{H}.d\vec{B}$. Where $\vec{H}$ is the magnetic fluid intensity (A.m^{-1}) and $\vec{B}$ is the induction,

For the adiabatic process $\delta Q = 0$,

$$dU = \vec{H}.d\vec{B} \tag{2.2}$$

Here, $\vec{B}$ = μ_0 $(\vec{H} + \vec{\mathrm{M}})$, Where $\vec{\mathrm{M}}$ is the magnetization and μ_0 = 4π x 10^{-7} is the permeability of the free space.

Substituting the value of $\vec{B}$ in equation (2.2) with integration by parts shows that cyclic increase of the internal energy can be written as

$$\Delta U = -\mu_0 \oint \vec{M}\, dH \tag{2.3}$$

Equation 2.3 shows that when magnetization lags the field, above integration gives the positive result which indicates conversion of magnetic work to internal energy.

We can write magnetization in terms of complex ferro fluid susceptibility [4]

$$\chi = \chi' - i\chi''$$

With the resulting magnetic field

$$H(t) = H_0 \cos \omega t = Re\left[H_0 e^{i\omega t}\right] \tag{2.4}$$

The resulting magnetization is

$$\vec{M}(t) = Re[\chi H_0 e^{i\omega t}\ ] = H_0(\chi^{'}\cos\omega t + \ \chi^{''} sin\ \omega t) \quad (2.5)$$

In above equation $\chi^{'}$ is the in-phase component of χ and $\chi^{''}$ is the out-phase component ofχ.

Substituting the value of M to equation (2.3),

$$\therefore\ \Delta U = \ 2\mu_0\ H_0^2\ \chi^{''} \int_0^{2\pi/\omega} \sin\omega t\ \ dt \quad (2.6)$$

From the equation (2.6), we can say that only $\chi^{''}$ present in the equation, so it is called the loss component.

Now volumetric power dissipation, $P = f\ \Delta U$

Integrating the equation (2.6) and multiplying with frequency , $f = \omega/2\pi$

$$\therefore P = \mu_0\ \chi^{''} \pi\ f\ H_0^2 \quad (2.7)$$

Here $\chi^{''}$ must be depends on the parameter of the ferro fluid.

2.3 Theory of heating with time dependent material parameter

The relaxation equation for motion less fluid in an oscillatory field is [4],

$$\frac{\partial M(t)}{\partial t} = \frac{1}{\tau}\big(M_0(t) - M(t)\big) \quad (2.8)$$

Where , τ = Relaxation time,

M_0 = Equilibrium magnetization in the applied field

= $\chi_0\ H_0\ \cos\omega t\ = Re\ (\chi_0\ H_0\ e^{i\omega t}\ )$

χ_0 = Equilibrium susceptibility

Substituting the value of M_0 and $M(t)$ in equation (2.8) yields,

$$\chi = \frac{\chi_0}{1+i\omega t} \quad (2.9)$$

Here, $\chi_0\ = \ \chi_i \frac{3}{\xi}\ (\coth\xi - \frac{1}{\xi})$

Here ξ is Langevin parameter and χ_i is the initial susceptibility.

From the equation (2.9), we can say that complex susceptibility depends on the frequency. From which component of susceptibility are,

$$\chi^{'} = \frac{\chi_0}{1+(\omega t)^2}$$

$$\chi'' = \frac{\omega t}{1+(\omega t)^2}\ \chi_0 \qquad (2.9b)$$

Above relation is identical to the Debye spectra of polar molecules in the absence of constant field.

2.4 Relaxation process in magnetic field

In magnetic hyperthermia cancer, nanoparticles are introduced in to the tumor region which produces RF magnetic field to eliminate cancer cells in tumor region. Brown and Neel relaxation [5] are dominant in dissipation of the energy. Here we neglect eddy currents and resonance losses. When nanoparticles rotate in the medium, Frictional interaction occurs between the particles and the medium which dissipates the heat. This is called Brown relaxation. Neel relaxation occurs when magnetic particles remain stationary and magnetic moment rotates within the crystal. Maximum heat dissipates through Brown relaxation so Neel relaxation must not be allowed to be dominant for achieving higher heating rates.

The Brownian time constant is given by,

$$\tau_B = \frac{3\,\eta\,V_H}{K_B\,T} \qquad (2.10)$$

Where, η = Viscosity coefficient of the matrix fluid

K_B = Boltzmann constant

= 1.38 X 10^{-23} J K^{-1}

T= Absolute temperature (K)

V_H = Hydro dynamic volume of the particle

Equation (2.10) reveals that Brownian constant depends on both, the viscosity of the medium and hydrodynamic volume of V_H. Here V_H is larger than magnetic volume $V_M = 4\pi R^3/3$. V_H is assumed that $V_H = (1 + \delta/R)^3 V_M$, where δ is the thickness of the sorbed surfactant layer.

The Neel relaxation time is given by,

$$\tau_N = \frac{\sqrt{\pi}}{2}\ \tau_0\ e^{\frac{\Gamma}{\sqrt{\Gamma}}} \qquad (2.11)$$

Where, $\Gamma = \mathcal{K}\,V_M/K_B\,T$, $\mathcal{K}$ is the anisotropy constant.

In the equivalent form, $\tau_N = \frac{\sqrt{\pi}}{2}\ \tau_D\ e^{\frac{\Gamma}{\Gamma^{3/2}}}$ (2.12 a)

$$\tau_D = \Gamma\ \tau_0 \quad (2.12\ b)$$

A typical ferro fluid has a broad distribution of particle size with a mean size 10 nm. In relaxation process, both Brownian and Neel relaxation occur in same time, the effective relaxation time τ is given by,

$$\frac{1}{\tau} = \frac{1}{\tau_B} + \frac{1}{\tau_N} \quad (2.13)$$

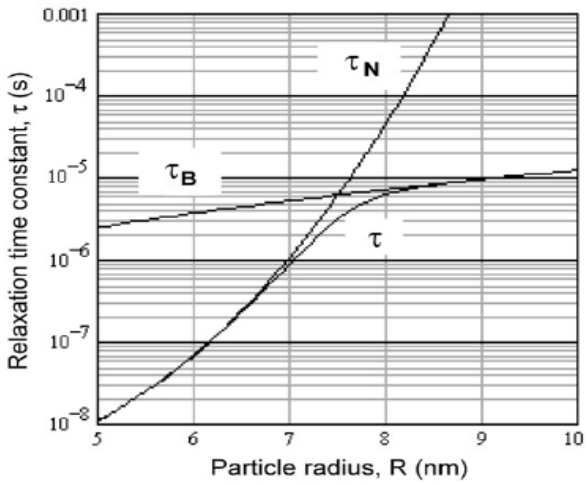

Figure 2.1: Time constant vs particle size for magnetic particle

Figure 2.1 shows that shorter time constant is dominant in determining the effective relaxation time for given size of nanoparticles.

From the equation (2.7) and (2.9 b), power dissipation

$$P = \pi\ \mu_0\ \chi_0\ \ H_0^2\ f\ \frac{2\pi f\tau}{1+(2\pi f\tau)^2} \quad (2.14)$$

Equation (2.14) is the power dissipation density for mono dispersed particle. Susceptibility χ_0 depends on the magnetic field but here assume that it is constant. It is assumed that χ_0 is the chord susceptibility corresponding to Langevin equation $L\ (\xi) = \vec{M}/M_s = \coth\xi - \frac{1}{\xi}$

Where $\xi = \ \mu_0\ M_d\ H\ V_M/K_B\ T$

$$M_s = \emptyset\, M_d$$

Here M_d is the domain magnetization of suspended particle and $\emptyset$ is the volume fraction solid.

Temperature rise for monodispersion particle as $\Delta T = P\,\Delta t/c$. Where c is the ferrofluid specific heat and Δt is the duration of heating.

CHAPTER 3

INTRODUCTION TO FINITE ELEMENT METHOD

3.1 Introduction

Engineering and physics problems can be defined through system of partial differential equation (PDE). It is easy to solve simple partial differential equations analytically like Poisson equation, Heat equation etc. But partial differential equation can't be that simple in engineering and physics problem. It is difficult to solve such a partial differential equation analytically. For such a complex partial differential equation, it is necessary to obtain approximate solution of the PDE's rather than the exact solution. Computational fluid dynamics known as CFD uses numerical methods and algorithms to solve these partial differential equations. Computers perform million of calculation to perform and give the numerical simulation of the fluid and heat transfer problem.

In back 1940s, finite difference method was used to find the solution for partial differential equations. For irregular geometries and for unusual specification of the boundary condition, this method is difficult to use. The difficulties associated with finite difference method inspired scientists to develop finite element method.

3.2 Finite element method: Background

The finite element method is a numerical technique to obtain approximate solution of partial differential equation in wide variety of engineering and physics problem. Essentially it gives a consistent technique for modeling the domain as a whole or geometry as an assembly of discrete parts.

In late 1950s, Finite element method was developed in structure and aircraft problem. In 1973, publication of Strang and Fix's [6] '*An Analysis of Finite Element Method'* gave strong mathematical foundation to this method and from there, this method emerged as one of the

most powerful numerical modeling techniques used in a wide variety of a engineering discipline e.g. structure mechanics, fluid dynamics, heat conduction, electromagnetism etc. This method has been accepted in different fields in engineering and physics problems due to its good attributes like ability to handle complex geometries, ability to treat different kinds of boundary conditions, easy programmability and sound mathematical foundation. An important feature of this method is that it has the ability to form a solution for individual elements before putting them together to represent the entire problem solution so that complex geometry or domain reduces to a series of simplified problems.

In the past, finite element method was synonymous with Galerkin finite element method. Galerkin finite element method is highly successful in different engineering areas and this method is based on the method of weight residual. First step in Galerkin finite element method is to convert partial differentials equation in to weak statement. One then applies some constrains to the given weak statement to characterize a finite set of basic functions. It produces symmetric stiffness matrix and here, the difference between exact solution of PDE's and approximate finite element solution is minimized with respect to energy norms.

3.3 Procedure of the finite element method

Regardless of the approach used to find the element properties, finite element method always uses step by step procedure to solve the given partial differential equation. Below is the step by step procedure that gives a general idea of how this method works [7].

- *Discretize the continuum*

The first step in finite element method is to divide given geometry or domain into different elements. A variety of element shapes like triangle, rectangle, tetrahedral etc can be used to divide a given domain. However engineering judgment is necessary for selecting the element that uses to divide the domain.

- *Select the interpolation function*

Once domain has been devide, the next step is to give the node numbers to each element and select the interpolation function for them. Interpolation function can be scalar,

vector or polynomials. The degree of polynomials chosen depends upon the number of nodes assigned to the element and number of unknown of the nodes.

- *Find the element properties*

Once element and its interpolation function have been selected, we need to define the matrix equation expressing the properties of individual elements. The matrix equation can be selected by different approaches like direct approach, variation approach or weight residual approach.

- *Assemble the element properties*

The next task in the finite element method is to assemble the element stiffness matrix. In the assembly, at a node where elements are interconnected, the value of the field variable must be the same for each element sharing the node. This is the important feature of the assembly procedure.

- *Imposed the boundary condition*

Now system equations are almost ready to solve the problem but we need to make changes in the equation as per the given boundary condition. We give known values as per the boundary condition to the dependent node.

- *Solve the system equation*

After assembly of the matrix and applying the boundary condition to the given problem, now we must solve a set of linear or non linear algebraic equations.

- *Post Processing*

Solutions obtained through above define procedures sometimes can be used to calculate some important parameters. Examples, in a heat conduction problem, once we find the temperature for a given problem it can be used to find the heat flux.

CHAPTER 4

BIO HEAT MODEL AND FINITE ELEMENT IMPLEMENTATION

4.1 Bio heat model

Heat transfer in biological tissue is normally done by blood supply governed by the distributed arterial and venous branching conduits. Dimension of the arterial conduits depends in so many parameters [8] like human age and health and is under homeostatic control which is difficult to understood and also it is difficult to describe it analytically. Arterial dimension vary dynamically and conservatively under feedback control, based on the local metabolic needs of tissue.

To solve this problem, many people developed modified pennes' equation. Chen and Holmes [9] gave heat transfer between blood and tissue in three modes. In the first mode, equilibrium of blood temperature with tissue temperature is represented by perfusion term that used in pennes' equation. Second mode related to heat transfer taking place when there is a temperature gradient between flowing blood and tissue temperature. The last mode reflects the heat transfer due to the small temperature fluctuation about the tissue temperature gradient of "nearly equilibrated" flowing blood. Weinbaum and jiji [10]considered a control volume of the tissue surrounding a pair of thermally significant blood vessels directly connected by capillaries. Baish introduced vascular tissue as composite with blood vessels acting like conductive fibers immersed in less conductive matrix, the surrounding tissue. Therefore there are so many controversies related to the Pennes model describing the bio-heat equation in regimes. Nonetheless whole organ, where, discrepancies between a pennes' and other model prediction are not necessarily of overriding concern. [10], [11].

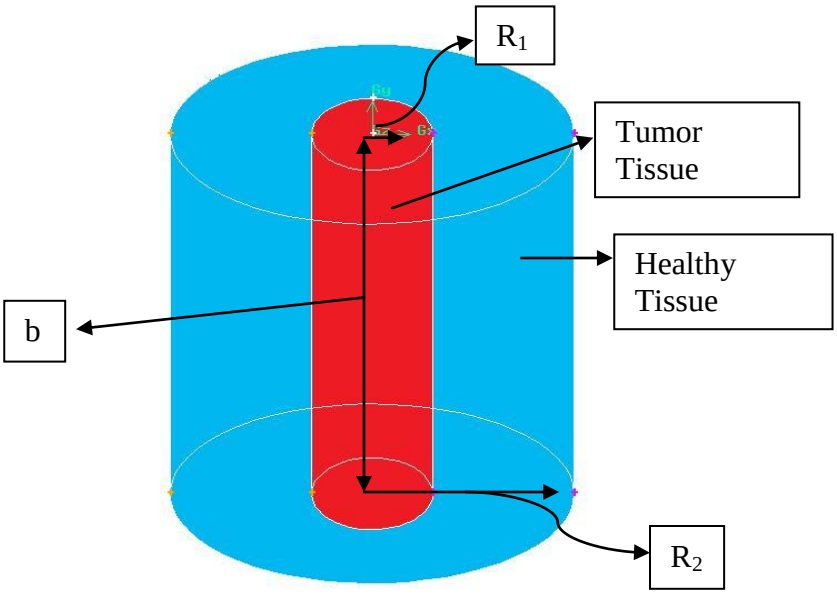

Figure 4.1: Composite Tissue Model

In our model, we consider two concentric cylinders representing tumor and healthy tissue as shown in the figure 4.1. Tumor tissue is taken with height b and radius r_1. Surrounding this cylinder, are represent healthy tissue with radius r_2 and height b. The bio-heat equation for the tumor tissue is representing by the equation [15]:

$$\rho_1 c_1 \frac{\partial T_1}{\partial t} = k_1 \frac{1}{r} \frac{\partial}{\partial r}\left[r \frac{\partial T_1}{\partial r}\right] + k_1 \frac{\partial^2 T_1}{\partial Z^2} + \omega b_1 c b_1 (T_{art} - T_1) + P(T_1)$$

where, $P(T_1) = \pi \mu_0 \chi_0 H_0^2 f \frac{2\pi f\tau}{1+(2\pi f\tau)^2}$

The bio-heat equation for healthy tissue is represented by equation:

$$\rho_2 c_2 \frac{\partial T_2}{\partial t} = k_2 \frac{1}{r} \frac{\partial}{\partial r}\left[r \frac{\partial T_2}{\partial r}\right] + k_2 \frac{\partial^2 T_2}{\partial Z^2} + \omega b_2 c b_2 (T_{art} - T_2)$$

In above equation, ρ_1 and ρ_2 are the density of tumor tissue and healthy tissue respectively. c_1 and c_2 are the specific heat capacities of tumor and healthy tissue respectively. In the right hand side of the equation, first and second term represents the temperature gradient in axial and radial direction. ωb_1 and ωb_2 are the volumetric perfusion rate of tumor and healthy tissue respectively. Third term in both the equation represents the heat sink term where T_{art} is arterial

temperature. Normally T_{art} is consider body normal temperature which is justified if there is no heat transfer taking place between arterial blood and surrounding tissue before capillaries reached.

In mathematical terms, a basic assumption of the Pennes model is that thermal equilibrium X_{eq} or the distance it takes before the blood in vessel reaches thermal equilibrium with surrounding tissue is infinite everywhere , except in the the capillaries where X_{eq} =0. Only the thermal equilibrium of the larger vessels can be defined with heat sink term. Heat transfer with smaller model require different model.

For the proposed model, the equations define the transient heat transport in the tumor and healthy tissue respectively. To simplify, the characteristic coefficients are taken to be independent of the position within the region. This model enables the study of the non-localized transient temperature behavior in tissue wherein fluctuation in the heat flux and temperature extend throughout many physiological regions where perfusion, density, specific heat and metabolic heat generation can vary.

4.2 Boundary condition

As the living systems are very complex, it is very difficult to find appropriate boundary conditions. Also boundary conditions are neither constant nor periodic. Boundary conditions for bio-heat equation for tumor tissue and healthy tissue are also different for various bio-medical applications. In our model, we use low Curie temperature nanoparticles that control the temperature profile. However it is still interesting to investigate the effect of various type of boundary condition on heat generation and dissipation which lead to corresponding distinct temperature profile. In our model we consider two types of boundary conditions: first is isothermal boundary condition and second is adiabatic boundary condition on the low Curie temperature controlled magnetic fluid hyperthermia.

- *Adiabatic boundary condition*

At the interface of tumor and healthy tissue, temperature and heat flux are continuous. So at the interface of disease and healthy tissue, temperature and heat flux conditions are describe by following expression [16].

$$T_1\,(r_1, z, t) = T_2\,(r_2, z, t) \tag{4.1}$$

$$k_1\,\frac{\partial T_1\,(r_1,z,t)}{\partial r} = k_2\,\frac{\partial T_2\,(r_2,z,t)}{\partial r} \tag{4.2}$$

Here we are selecting the adiabatic boundary condition. The reason behind selecting this adiabatic condition is that temperature field is not affected by centre domain or external heating to the position far from the centre domain. There is no heat transfer taking place far from the centre of the domain. In this case, there is no heat leaving from the top of the tissue surface. The boundary condition for this case:

$$\frac{\partial T_1(r,b,t)}{\partial z} = \frac{\partial T_2(r,b,t)}{\partial z} = 0 \tag{4.3}$$

Here b = top surface of the tumor and healthy tissue

At the bottom of the healthy and disease tissue, z=0:

$$\frac{\partial T_1(r,0,t)}{\partial z} = \frac{\partial T_2(r,0,t)}{\partial z} = 0 \tag{4.4}$$

At the outer surface of the healthy tissue $r = r_2$:

$$\frac{\partial T_2(r_2,z,t)}{\partial r} = 0 \tag{4.5}$$

- *Isothermal Boundary Condition*

At the position far from the centre of the domain, temperature will remain constant that is temperature of top and bottom surface of the cylinder tissue must match the core body temperature. Also outer body temperature of the healthy tissue is equal to the body normal temperature.

At the bottom side of the composite tissue, the boundary condition is:

$$T_1(r,0,t) = T_2(r,0,t) = T_0 \quad (4.6)$$

At the top side of the composite tissue, the boundary condition is:

$$T_1(r,b,t) = T_2(r,b,t) = T_0 \quad (4.7)$$

At the outer surface of the healthy tissue, boundary condition is:

$$T_2(r_2,z,t) = T_0 \quad (4.8)$$

Here we neglect the thermo regulation mechanism of the biological bodies which induced slight temperature.

- *Initial condition:*

Before applying AC magnetic field to the tumor tissue, the temperature of the body is equal to the body core temperature. Therefore, initial condition prior to the application of the ac magnetic field is given by:

$$T_1(r,z,0) = T_2(r,z,0) = T_0 \quad (4.9)$$

Here, z=height of the composite tissue

b= Top surface of the composite tissue

T_0= Body core temperature

4.3 Finite element procedure and its computer implementation

In this section, finite element procedure for Pennes bio-heat equation is explained. Also computer code for this finite element procedure is explained with appropriate part..

4.3.1 Finite Element Procedure

The finite element procedure has been explained for the Pennes bio-heat equation. Pennes bio heat equation in two dimensions is:

$$\rho_1 c_1 \frac{\partial T_1}{\partial t} = k_1 \frac{1}{r} \frac{\partial}{\partial r}\left[r \frac{\partial T_1}{\partial r}\right] + k_1 \frac{\partial^2 T_1}{\partial Z^2} + \omega b_1 cb_1 (T_{art} - T_1) + P(T_1) \quad (4.10)$$

$$\rho_2 c_2 \frac{\partial T_2}{\partial t} = k_2 \frac{1}{r} \frac{\partial}{\partial r}\left[r \frac{\partial T_2}{\partial r}\right] + k_2 \frac{\partial^2 T_2}{\partial Z^2} + \omega b_2 cb_2 (T_{art} - T_2) \quad (4.11)$$

Equation (4.10) and (4.11) are related to Pennes bio-heat equation related to tumor and healthy tissue respectively. Here in this section, finite element procedure for tumor tissue has been explained in detail. Therefore governing equation for finite element procedure:

$$\mathcal{L}(T) = \rho_1 c_1 \frac{\partial T_1}{\partial t} - k_1 \frac{1}{r} \frac{\partial}{\partial r} \left[r \frac{\partial T_1}{\partial r} \right] - k_1 \frac{\partial^2 T_1}{\partial Z^2} - \omega b_1 cb_1 (T_{art} - T_1) - P(T_1) = 0 \tag{4.12}$$

We first approximate the given governing equation $T(x, y)$ by $\tilde{T}(x, y)$, which has the form:

$$\tilde{T} = \sum_{i=1}^{m} N_i \tilde{T}_i(x, y) \tag{4.13}$$

Here N_i is the element interpolation function and m is the number of nodes per element.

The first step is to choose the interpolation function or weighting function for given governing equation. In Galerkin finite element method, weighting function has been chosen same as approximating function i.e. $w_j(x, y) = N_j(x, y)$. Applying weighting function to the equation (4.12) and writing equation to the integral form:

$$\int_\Omega N_i \left[\rho_1 c_1 \frac{\partial T_1}{\partial t} - k_1 \frac{1}{r} \frac{\partial}{\partial r} \left[r \frac{\partial T_1}{\partial r} \right] - k_1 \frac{\partial^2 T_1}{\partial Z^2} - \omega b_1 cb_1 (T_{art} - T_1) - P(T_1) \right] 2\pi r \, dr \, dz = 0 \tag{4.14}$$

Here Ω is the domain and N_i is the interpolation function

$$\int_\Omega N_i \left[\rho_1 c_1 \frac{\partial T_1}{\partial t} \right] 2\pi r \, dr \, dz - \int_\Omega N_i \left[k_1 \frac{1}{r} \frac{\partial}{\partial r} \left[r \frac{\partial T_1}{\partial r} \right] + k_1 \frac{\partial^2 T_1}{\partial Z^2} \right] 2\pi r \, dr \, dz -$$

$$\int_\Omega N_i \left[\omega b_1 cb_1 (T_{art} - T_1) \right] 2\pi r \, dr \, dz - \int_\Omega N_i \left[P(T_1) \right] 2\pi r \, dr \, dz = 0 \tag{4.15}$$

In equation (4.15) involving second order term:

$$\int_\Omega N_i \left[k_1 \frac{1}{r} \frac{\partial}{\partial r} \left[r \frac{\partial T_1}{\partial r} \right] + k_1 \frac{\partial^2 T_1}{\partial Z^2} \right] 2\pi r \, dr \, dz \, . \tag{4.16}$$

Solving equation (4.16) by integration by parts and writing in the matrix form,

$$[K_c] = \frac{\pi . k_1 . (r_1 + r_2 + r_3)}{6.A} \begin{bmatrix} b_1^2 + c_1^2 & b_1 . b_2 + c_1 . c_2 & b_1 . b_3 + c_1 . c_3 \\ & b_2^2 + c_2^2 & b_2 . b_3 + c_2 . c_3 \\ & & b_3^2 + c_3^2 \end{bmatrix} \quad (4.17)$$

Therefore $[K_c]$ is the symmetric matrix.

In above matrix, r_1, r_2, r_3 are the co-ordinates of triangular element in r direction.

Also, $b_1 = z_2 - z_3$, $b_2 = z_3 - z_1$, $b_3 = z_1 - z_2$

$c_1 = r_3 - r_2$, $c_2 = r_1 - r_3$, $c_3 = r_2 - r_1$

Here, $x_1, x_2, x_3, y_1, y_2, y_3$ are the co-ordinates of the triangular element.

Rewriting the equation (4.15) in the matrix form:

$$[c]^e \left\{\frac{dT}{dt}\right\}^e + [K_c]^e \{T\}^e + [K_w]^e \{T\}^e = \{T_{art}\}^e + \{P_1\}^e \quad (4.18)$$

Where,

$[c] = \int_\Omega N_i \, \rho_1 \, c_1 \, 2\pi r \, dr \, dz$

$[K_w] = \omega b_1 \, cb_1 \int_\Omega N_i \; 2\pi r \, dr \, dz$

$\{T_{art}\} = T_{art} \int_\Omega N_i \; 2\pi r \, dr \, dz$

$\{P_1\} = P(T_1) \int_\Omega N_i \; 2\pi r \, dr \, dz$

In equation (4.18), we neglect to write boundary condition term because of the isothermal boundary condition and adiabatic boundary condition at the tissue surface. Value of this natural boundary condition is zero at the surface of the tissue .The coefficient matrix $[c]$ of the time derivative of the nodal temperatures is the element capacitance matrix. The coefficient matrices $[K_c]$ are element conductance matrix. $\{T_{art}\}$ and $\{P_1\}$ are load vector arising from perfusion and due to the magnetic heat generation respectively. After we select the element shape and an appropriate set of interpolation function; we can evaluate this equation and assemble them for an aggregate element representing the whole solution domain.

Equation (4.18) has first order time derivative term so it is difficult to solve first order term directly because it will introduce unstable solution or asymmetric matrix. One way of avoiding this difficulty is to solve this first order term using time marching (Crank-Nicolson method).

4.3.1.1 Crank-Nicolson Method

Partial differential equation (4.18) should be integrated with respect time to obtain the transient solution. It is not possible to integrate this equation as it leads to instability and asymmetric matrix. Therefore further more approximation is required in time to obtain a set of algebraic equation in terms of nodal temperatures. The most common used time integration method for equation (4.18) is called the θ family of approximation also called Crank-Nicolson method. In this method, time derivative can be split either explicitly or implicitly[6].

- *Explicit method*

In explicit method, forward difference scheme has been applied to the time derivative.

$$\therefore \frac{dT}{dt} = \frac{T^{n+1} - T^n}{\Delta t} \tag{4.19}$$

Substituting the value of (4.19) in to (4.18),

$$\therefore [c]\left[\frac{T^{n+1} - T^n}{\Delta t}\right] + [K_c]\{T\} + [K_w]\{T\} = \{T_{art}\} + \{P_1\} \tag{4.20}$$

$$\therefore [c][T^{n+1} - T^n] + \Delta t[K_c]\{T\} + \Delta t\,[K_w]\{T\} = \Delta t[\{T_{art}\} + \{P_1\}] \tag{4.21}$$

$$\therefore [c]\,T^{n+1} = T^n + \Delta t[\{T_{art}\} + \{P_1\}] - \Delta t\{[K_c]\{T\}^n + [K_w]\{T\}^n\} \tag{4.22}$$

From equation (4.22), we can say that once having known value of temperature for n time steps, temperature T at all nodes at time level n+1 are calculated. Same procedure is used to calculate the temperature at time level n+2 using the known values at n+1. In this way, solution is progressively obtained by marching in time steps.

Explicit method is relatively simple and also we find the solution with low memory requirements. However for complicated geometry, explicit method is not best choice. For given

Δx, there is some critical value of Δt beyond which solution is unstable. Δt must be less than some limit which is imposed by stability analysis. In this case, Computer takes long running time to make calculation.

- *Implicit method*

In Implicit method, backward difference scheme has been applied to the given partial differential equation.

$$\therefore [c]\left[\frac{T^{n+1}-T^{n}}{\Delta t}\right]+[K_c]\{T\}^{n+1}+[K_w]\{T\}^{n+1}=\{T_{art}\}+\{P_1\} \quad (4.23)$$

$$\therefore [c]\{T\}^{n+1}-[c]\{T\}^{n}+\Delta t\left[[K_c]\{T\}^{n+1}+[K_w]\{T\}^{n+1}\right]=\Delta t[\{T_{art}\}+\{P_1\}]^{n+1} \quad (4.24)$$

In equation (4.24) shows that property at n time steps on the right hand side and properties at n+1 time steps are on the left hand side. Once we formulate the equation in implicit method as shows in equation (4.25), we can find the temperature for n+1 time steps by set of algebraic equation.

Implicit method involves manipulations of large matrices; it involves complex set of calculations than explicit approach. However stability can be maintained over much larger values of Δt. So less computer time is required for calculation. Implicit method is used for complicated geometry. Since Δt can be the large in the implicit method, Truncation error is also large so implicit method that follows the transient behavior may not be as accurate as explicit method but here relative time wise inaccuracy is not important.

We can write both explicit and implicit form of equation in a common form that is called θ method [6].

$$[c]+\theta[\Delta t([K_c]+[K_W])\{T\}^{n+1}=([c]-(1-\theta)(\Delta t([K_c]+[K_W])\{T\}^{n}+\Delta t(\{T_{art}\}+\{P_1\})^{n} \quad (4.25)$$

For the different value of the θ in equation (4.25), we can get the different equation schemes:

θ=0, the forward difference method (conditionally stable)

θ=1, the backward difference method (unconditionally stable)

θ=0.5, the Crank-Nicolson method (unconditionally stable)

For $\theta \geq 0.5$, equation (4.25) is stable and for $\theta \leq 0.5$,equation (4.25) is conditionally stable.

For the forward difference method, the stability requirement is[6],

$$\Delta t < \Delta t_{cr} = \frac{2}{(1-2\theta)\lambda_{max}} , \theta < 0.5$$

Where, λ_{max} is the largest eigenvalue of the system.

4.3.2 Computer Implementation

Simulation of finite element method required mesh data first. It is therefore crucial to read the mesh and element data from the source file and allocate proper memory to given data in appropriate way. For this, mesh and element connectivity data can be read and stored as shown in below:

```
fid = fopen('m.txt', 'r');
data1 = textscan (fid, '%*d %*d %*d %d %d %d',10000, 'headerlines',0);

%% Node co-ordinates
fid = fopen('n.txt', 'r');
data2 = textscan(fid, '%*f %f %f',5000, 'headerlines',0);

%% Boundry layer node
fid=fopen('b.txt','r');
data3=textscan(fid, '%d',200, 'headerlines',0);

%% Element and node table
M=[data1{1} data1{2} data1{3}];
N=[data2{1} data2{2}];
O=[data3{1}];
%% element and node size
[m1,m2]=size(M);
[n1,n2]=size(N);
[o1,o2]=size(O);
```

There are different physical parameters associated with the given partial differential equation. So it is necessary to define and allocate memory for those parameters. Here these physical parameters are defined in the programme globally as shown below.

```
%% Physical parameter
rho1=1.1*10^3;
rho2=1*10^3;
c11=4.2*10^3;
k11=0.55;
k22=0.5;
wb1=1;
cb1=4.2*10^3;
Tart=37;
%% Parameter for energy dissipation term
tau0=10^-9;
Kans=23*10^3;
Vm=1.4367*10^-24;
Kb=1.38*10^-23;
T0=37;
mu0=4*pi*10^-7;
Md=446*10^3;
H=6500;
w=3.14159*10^6;
```

4.3.2.1 Local Stiffness Matrix and Assembly Procedure

It is necessary to define the local stiffness matrix and load vector. Before defining the local stiffness matrix and load vector, it is crucial to allocate the memory for that stiffness matrix. Once you allocate the memory for the stiffness matrix and load vector, it is easy for the computer to find the data related to stiffness matrix and load vector. Below is the memory allocation for the stiffness matrix and load vector.

```
%% Initialize the stiffness matrix and load vector
K4=zeros(n1,n1);
K3=zeros(n1,n1);
F1=zeros(n1,1);
F2=zeros(n1,1);
```

Once memory has been allocated to the stiffness matrix and load vector, next step is to define the local stiffness matrix and load vector to the individual element.

```
%% Stiffness matrix
k1=((2*pi*k)/(12*A))*[((b1^2)+(c1^2)) (b1*b2+c1*c2) (b1*b3+c1*c3);(b1*b2+c1*c2)
((b2^2)+(c2^2)) (b2*b3+c2*c3);(b1*b3+c1*c3) (b2*b3+c2*c3) ((b3^2)+(c3^2))]*(r1+r2+r3);


k2=((wb1*cb1*2*pi*A)/60)*[(6*r1+2*r2+2*r3) (2*r1+2*r2+r3) (2*r1+r2+2*r3);(2*r1+2*r2+r3)
(2*r1+6*r2+2*r3) (r1+2*r2+2*r3);(2*r1+r2+2*r3) (r1+2*r2+2*r3) (2*r1+2*r2+6*r3)];
```

```
k3=((rho*c11*2*pi*A)/60)*[(6*r1+2*r2+2*r3) (2*r1+2*r2+r3) (2*r1+r2+2*r3);(2*r1+2*r2+r3)
(2*r1+6*r2+2*r3) (r1+2*r2+2*r3);(2*r1+r2+2*r3) (r1+2*r2+2*r3) (2*r1+2*r2+6*r3)];
   k4=k1+k2;

 %%Load vector
   f1=((wb1*cb1*Tart*2*pi*A)/12)*[(2*r1+r2+r3);(r1+2*r2+r3);(r1+r2+2*r3)];

f2=((2*pi*p*A)/12)*[(2*r1+r2+r3);(r1+2*r2+r3);(r1+r2+2*r3)];
```

After defining the local stiffness matrix and load vector to the each element, it is necessary to assemble local stiffness matrix and load vector to create global matrix and load vector depending upon the nodal data and element connectivity data. Assembly procedure can be defined in the following way.

```
%Assemble the matrix
   for i=1:m2
      for j=1:m2
      K4(M(e,i),M(e,j))=k4(i,j)+K4(M(e,i),M(e,j));
      K3(M(e,i),M(e,j))=k3(i,j)+K3(M(e,i),M(e,j));
      end
   end
   for i=1:m2
      F1(M(e,i),1)=f1(i,1)+F1(M(e,i),1);
      F2(M(e,i),1)=f2(i,1)+F2(M(e,i),1);
   end
end

for i=265:489
   F2(i,1)=0;
end
```

4.3.2.2 Initialize the Matrix

As problem is time dependent, it is necessary to define the appropriate initial condition to the bio-heat equation. This step is defined below as:

```
for i=1:n1
    TT(i)=37;
end
```

4.3.2.3 Time Marching

In order to get the temperature distribution for every time steps, explicit method has been used. Here saturation magnetization for low Curie temperature cannot assume to be constant. In fact saturation magnetization depends on the temperature. Quick drop of saturation magnetization around the Curie temperature which directly leads to corresponding heat generation in self regulation MFH.So it is necessary to updating the value of M_s for every time steps.

Here Saturation magnetization can be found using the relation of hyperbolic tangent function as shown below [18].

$$\frac{M_s(T)}{M_s(T_0)} = \tanh\left[\frac{M_s(T)/M_s(T_0)}{T/T_c}\right] \tag{4.26}$$

Equation (4.26) is non linear equation. So It is difficult to find the value of saturation magnetization directly from this equation. In order to find the value of saturation magnetization for every time step, here we used Newton-Raphson method. A better approximation for saturation magnetization can be made thorough formula.

$$M_s = M_s(0) - \frac{f(M_s(0))}{f'(M_s(0))} \tag{4.27}$$

Here $M_s(0)$ is the initial guess. One of the important things in Newton-Rapshon method is that function should be continuously differentiable and its derivative is non-zero at $f(M_s(0))$.

```
for j=1:264
    syms Ms1
    Mst0=1338;
    n=1200;
    Tc=48;
    fMs=(Ms1/Mst0)-tanh((Ms1*Tc)/(Mst0*T(j)));
    fMsd=diff(fMs,Ms1);
    f=Ms1-fMs/fMsd;
    for k=1:20
        ff=subs(f,Ms1,n);
        if ff==n
          ff;
          break
        else
```

```
            n=ff;
        end
    end
    Ms(j)=vpa(abs(ff));
```

From relaxation process in the magnetic field, energy dissipation of the nano particle depends on the saturation magnetization of the nanoparticles. So once saturation magnetization has been updated, it is necessary to update the value of energy dissipation term.

```
    Ms(j)=vpa(abs(ff));
    tau=tau0*exp((Kans*Vm)/(Kb*(T(j)+273)));
    zita=(mu0*Ms(j)*H*Vm)/(Kb*(T(j)+273)*fi);
    X0=((Ms(j))/H)*((coth(zita))-(1/zita));
    p1(j)=(mu0*X0*H^2*w^2*tau)/(2*(1+(w^2*tau^2)));
    F22(j)=F2(j,1)*p1(j)/p;
    F11(j)=F1(j,1);
```

Finally Boundary condition has been given to problem. Here Dirichlet boundary condition has been given.

```
Fload=F*delta_t-delta_t*K4*T+K3*T;
T=zeros(n1,1);
T=K3\Fload;
```

CHAPTER 5

NUMERICAL RESULTS

5.1 Introduction

In this section, Finite element results obtained by solving bio-heat equation in the context of magnetic fluid hyperthermia have been presented. Temperature distribution patterns over a tissue domain containing tumor have been computed for different boundary conditions (isothermal and adiabatic), different models (two region model and three region model) and for different blood perfusion rates. The finite element code used for computation has been validated by comparing its results for 2D Laplace equation and 1D bio heat equation. Results agree well with analytical solutions. The ability of finite element method to handle irregular geometries and irregular mesh structure has been underlined by obtaining results on irregular shaped domain using irregular mesh structure.

5.2 Laplace equation

The finite element code has been validated by solving 2-D Laplace equation and comparing the results with the analytical solution.

Laplace equation is a second order partial differential equation. Solution of the Laplace equation is important in many fields like fluid mechanics, solid mechanics and heat conduction. Solution of Laplace equation in heat conduction gives steady state temperature field. Solution of the Laplace equation is called harmonic function. In two dimensions, Laplace equation is defined as:

$$\frac{\partial^2 \varphi}{\partial x^2} + \frac{\partial^2 \varphi}{\partial y^2} = 0 \qquad (5.1)$$

This is often writing as, $\nabla^2 \varphi = 0$.

5.2.1 Test Problem

As a test problem, Laplace equation has been solved on a unit square domain with the boundary conditions:

$$\varphi(0, y) = 0, \quad \varphi(1, y) = 0,$$

$$\varphi(x, 0) = 0, \quad \varphi(x, 1) = 1$$

Exact solution of this Laplace equation is given as:

$$\varphi(x, y) = \sum_{n=1}^{\alpha} b_n \sin(n\pi x)\,(e^{n\pi y} - e^{-n\pi y}) \tag{5.2}$$

Where $b_n = \frac{2\,(1-(-1)^n)}{n\pi\,(e^{n\pi} - e^{-n\pi})}$

Contour profile of this Laplace equation is given below in the figure:

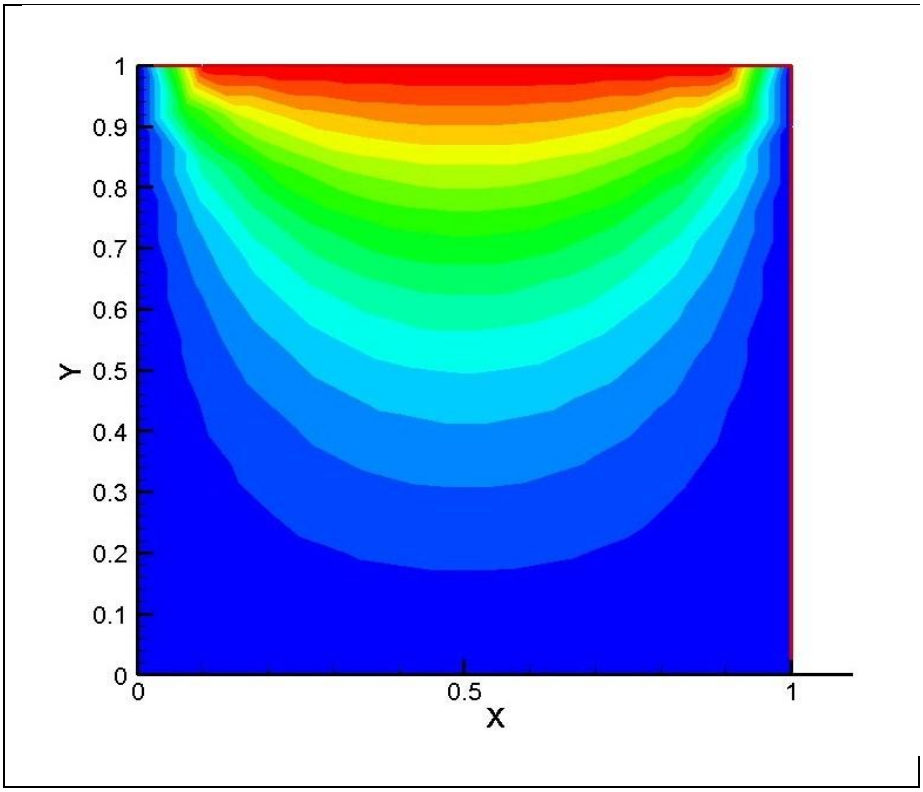

Figure 5.1: Contour profile for exact solution and laplace equation

Finite element solutions have been compared with exact solution in figure 5.2.

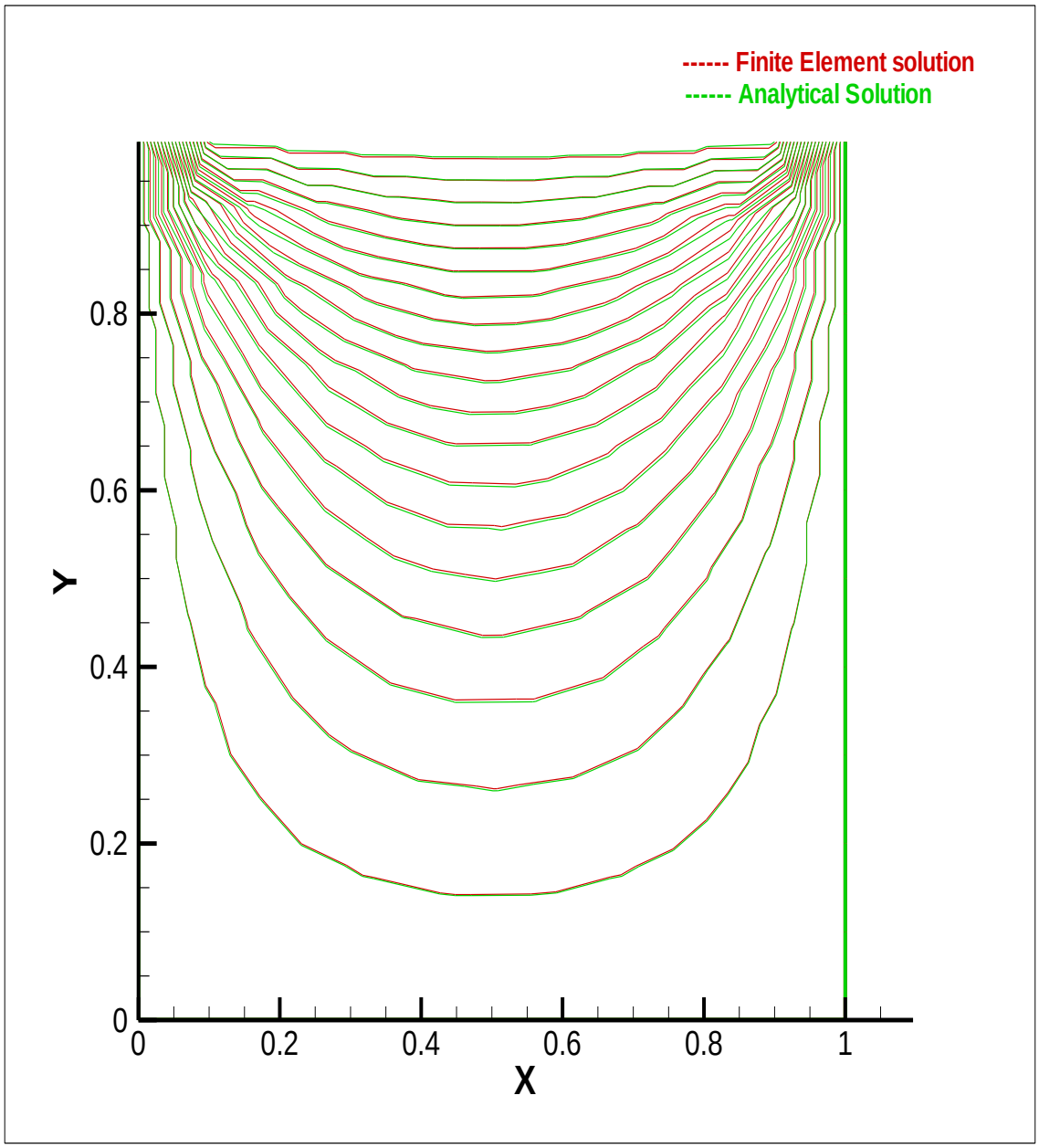

Figure 5.2: Comparison between exact solution and finite element solution of laplace equation

It can be observed that the finite element solution agrees well with the exact solution.

5.3 Bio heat equation

Transport of the thermal energy in the living tissue is complex processes which involve conduction, radiation, metabolism evaporation and phase change. So it is difficult to analyze all thermal phenomena significant in a tissue. After subjecting to various assumptions, Pennes derived the bio –heat transfer equation often called Pennes bio-heat equation.

The governing differential equation for the bio heat transfer problem is given as

$$\rho\, c_p \frac{\partial T}{\partial t} = \nabla . k \nabla T + \, c_p \, M \, (T_{art} \, - \, T) \tag{5.2}$$

Where T is the temperature, c_p is the specific heat, k is the thermal conductivity, ρ is the density, T_{art} is the body normal temperature.

Different kind of analytical solutions have been found for different cases. One such a case is time dependent heat conduction with 1-D rod of length L. The rod is insulated along the length L with the end temperature set to 0.

For simplicity, assuming T_{art} =0 .Therefore governing equation becomes

$$\frac{\partial T}{\partial t} = \alpha \, \frac{\partial^2 T}{\partial x^2} - \beta T \tag{5.3}$$

Where $\beta = \frac{M}{\rho}$ and $\alpha = \frac{k}{\rho \, c_p}$ .The above equation can be solved by separation of variable method.

The exact solution of equation (5.3) can be written as [19]

$$T(x,t) = \sum_{n=1}^{\alpha} A_n \; e^{-(\alpha[(n^2\pi^2)/(L^2)]+\beta)t} \; \sin\left(\frac{n\,\pi\,x}{L}\right)$$

In above equation, constant A_n is determined by the initial condition given in the problem. For this problem, initial condition is given as [19]

$$T(x,0) = V\left\{1 - \left[\left(\frac{2x}{L}\right) - 1\right]^2\right\}$$

Where, V is the maximum temperature. In this problem, Maximum temperature is 10.

An expression for the unknown constant is given as[19]

$$A_n = \frac{2}{L}\int_0^L T(x,0)\sin\left(\frac{n\pi x}{L}\right)dx$$

After further manipulation the following result is obtained[19]

$$A_n = \frac{V}{n^3\pi^3}\{16 - [16\ \cos(n\pi) + 8\,n\,\pi\ \sin(n\pi)\}$$

The accuracy of the 2-D finite element code was checked with analytical solution of bio-heat transfer equation. 2-D finite element code was used to solve bio-heat equation in the insulated rod with the following parameter listed in table 5.1

Table 5.1: Parameters for 1- D bio –heat transfer equation

L = 10.0
$T(0,t) = T(L,t) = 0$
$c_p = \rho = M = k = 1$
$T_{art} = 0$
$T(x,0) = V\left\{1 - \left[\left(\frac{2x}{L}\right) - 1\right]^2\right\}$
$\Delta t = 0.01$

The excellent match between the computed and analytical results is displayed in figure 5.3 below.

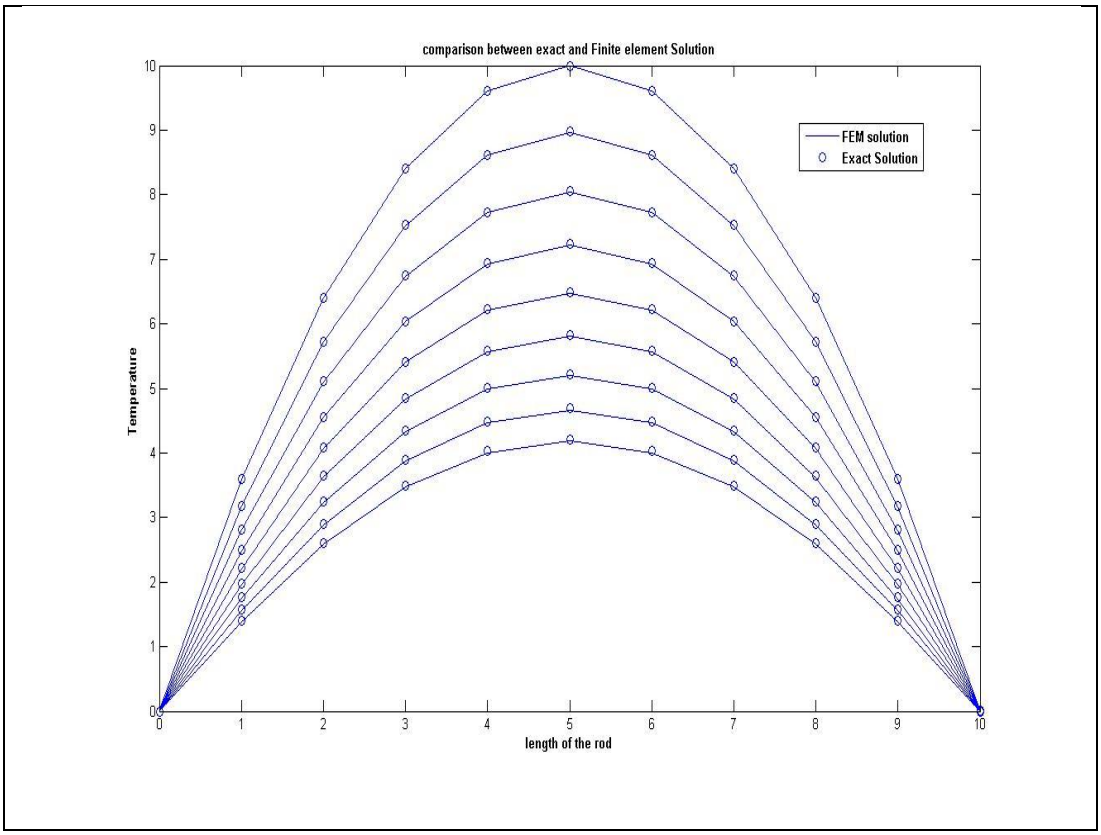

Figure 5.3: Comparison between Analytical and FEM solution for bio heat equation

5.4 Composite tissue model

5.4.1 Physical parameter

We define a composite tissue with r_1=1.5 cm, r_2=3.5 cm and z=3 cm, where r_1 and r_2 are the radii of tumor and healthy tissue respectively, and z is the height of the tissue. In our study, heating area is the whole tumor region which is localized by mono dispersed super magnetic particle with diameter of 14 nanometers. Although this magnetic particle doesn't give importance to the size of the magnetic particle but it is very important to choose critical size of the magnetic particle for the maximum heat generation which can decrease the demand of the nanoparticles and at the same time, side effects can be limited to the lowest level during the

therapy. The typical physiological properties for magnetic fluid hyperthermia treatment are given below in the table [20].

Table 5.2: Thermal properties of the composite tissue

$c_1 = c_2 = 4.2 \times 10^3$ J kg^{-1} °C^{-1}
$T_{art} = 37$ °C
$C_b = 4.2 \times 10^3$ J kg^{-1} °C^{-1}
$\rho_1 = 1.1$ g cm^{-3}
$\rho_2 = 1$ g cm^{-3}
$k_1 = 0.0055$ W cm^{-1}°C^{-1}
$k_2 = 0.005$ W cm^{-1}°C^{-1}
$\varphi = 0.003$

In the table c_1 and c_2 are the specific heat of tumor and healthy tissue, ρ_1 and ρ_2 are the density of tumor and healthy tissue, C_b is the specific heat of the blood, k_1 and k_2 are the thermal conductivity of the tumor and healthy tissue.

For the hyperthermia cancer, treatment temperature should be in the acceptable range in clinical practice. According to Rosensweig model, temperature depends on the higher frequency and amplitudes. Higher frequency leads to higher therapeutic temperature. Frequency and amplitude range for hyperthermia cancer are generally in the range of f=50 ~ 1200 kHz[22]. For our model, frequency f has been taken as 500 kHz and magnetic field strength H has been considered as 6500 kA/m.

Parameters that can be used to calculate the heat dissipation of the nanoparticles are given below in the table

.

Table 5.3: Heat dissipation parameters

$\tau_0 = 10^{-9}$ s
$\mu_0 = 4\pi$ x 10^{-7} Tm/A
K_b=1.38 x 10^{-23} JK^{-1}
Anisotropy ,K= 23 KJ/m^3
M_d= 446 kAm^{-1}
$V_M = \pi\ d^3/6$

5.4.2 Temperature Distribution

The temperature distribution in the tumor region and the healthy region are of great importance in this therapy. Here we analyze the temperature at the centre region of the tumor tissue and at the same time monitor heat increase in the healthy region. We predict the model for low curie nanoparticles evenly distributed in the centre of the tumor region. In the model, temperature distribution reaches to the steady state after 3000 second. Figure 5.4 depicts the temperature distribution at the blood perfusion rates of $\omega b_1 = \omega b_2 = 0.001$ g cm^{-3} $s^{1.}$Due to the isothermal boundary condition; edge of the cylindrical tissue is at constant temperature of 37℃ as shown in the figure 5.4. The maximum temperature of the centre region of the tumor tissue is at of 43 ℃. The reason behind maximum temperature at the centre of the tumor region is because the nanoparticle is evenly distributed in the centre of the tumor region.

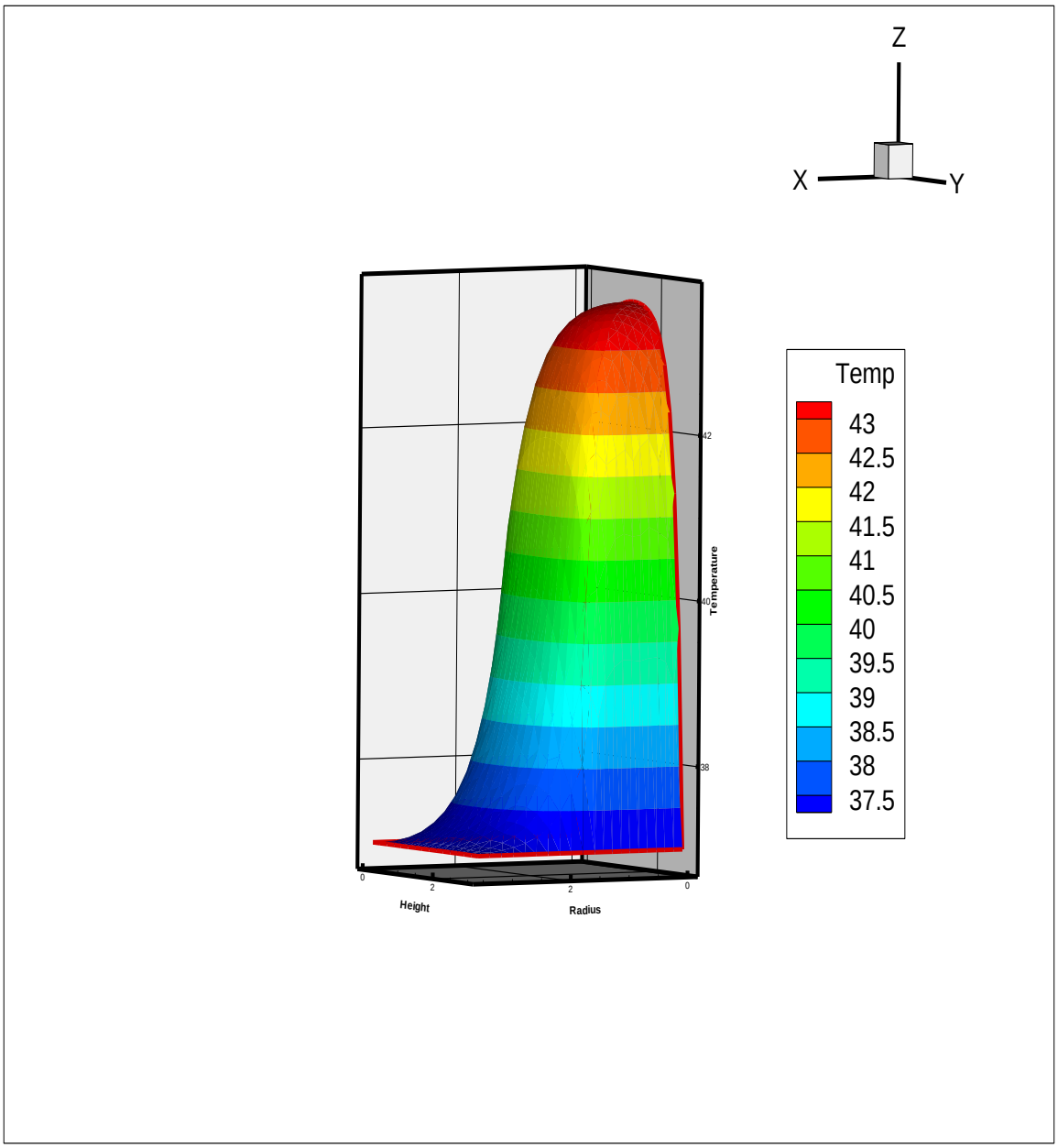

Figure 5.4: Temperature Distribution in composite tissue

Contour plot of the temperature distribution of the tumor and healthy region is shown in figure 5.5. It can be observed that nanoparticles distributed evenly in the centre region keep the temperature in the centre region in a range of 40℃ ~ 43℃ which is sufficient for the hyperthermia cancer therapy. Also it can be seen that the temperature of the healthy region is below 40℃ because there is no heat generation in the healthy region. A small amount of heat is

transferred from the tumor region to the healthy region because of the small difference in the conductivity of the both tissues. So there is a minimal damage to the healthy region.

Because of the isothermal boundary condition at the edge of the tissue, there is slight temperature change in the z direction. From the figure, it is clear that temperature is slightly less near the edge of the tissue compare to the centre region of the tumor tissue.

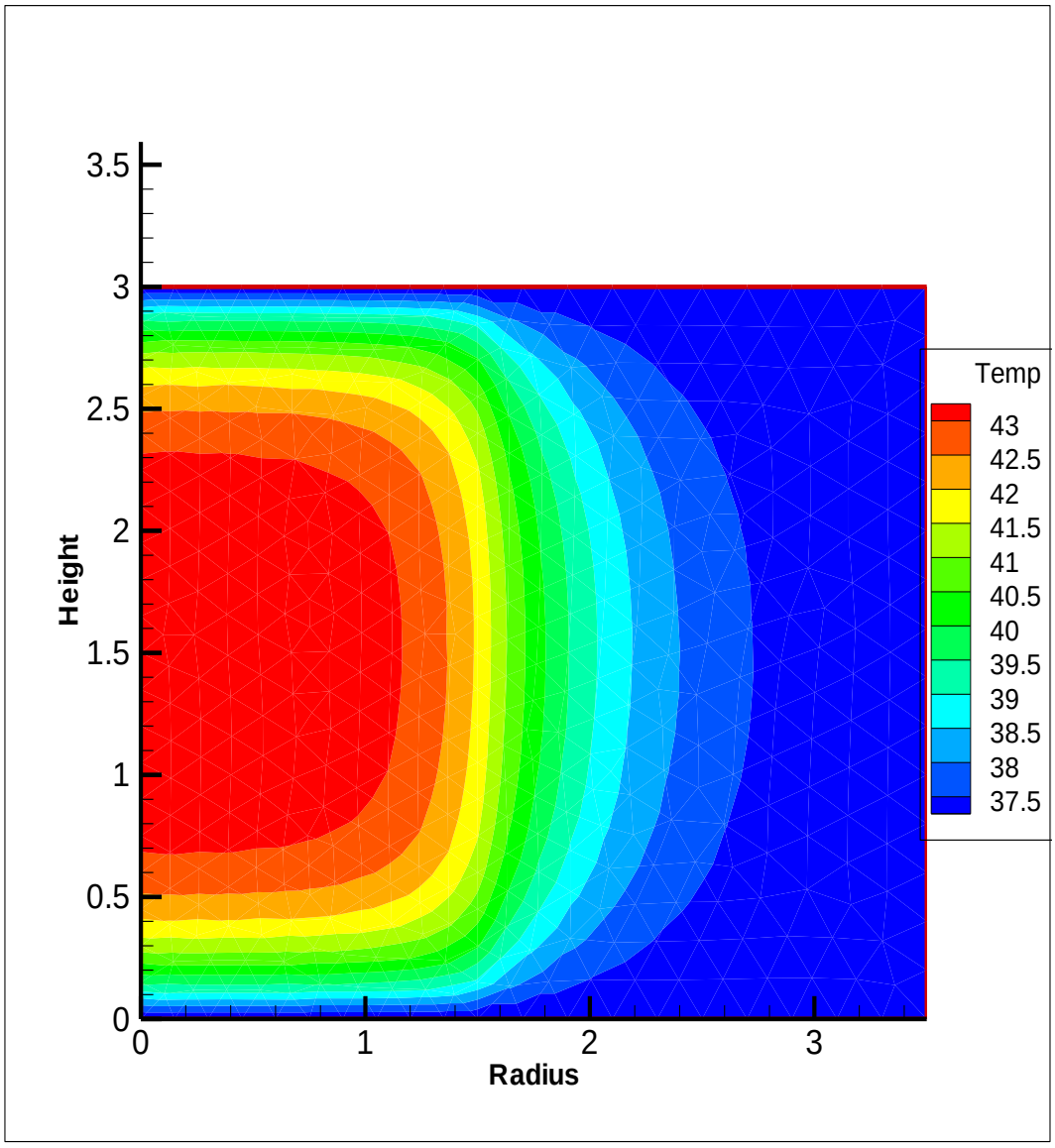

Figure 5.5: Contour plot of temperature distribution of tumor and healthy region

Temperature variation with radius at different heights z=0.5 cm and z=1.5 cm is shown in figure 5.6. Figure reveals that temperature decreases with increase in radius. Also temperature levels are slightly more at z=1.5 cm compared to levels at z = 0.5 cm because of the isothermal boundary condition.

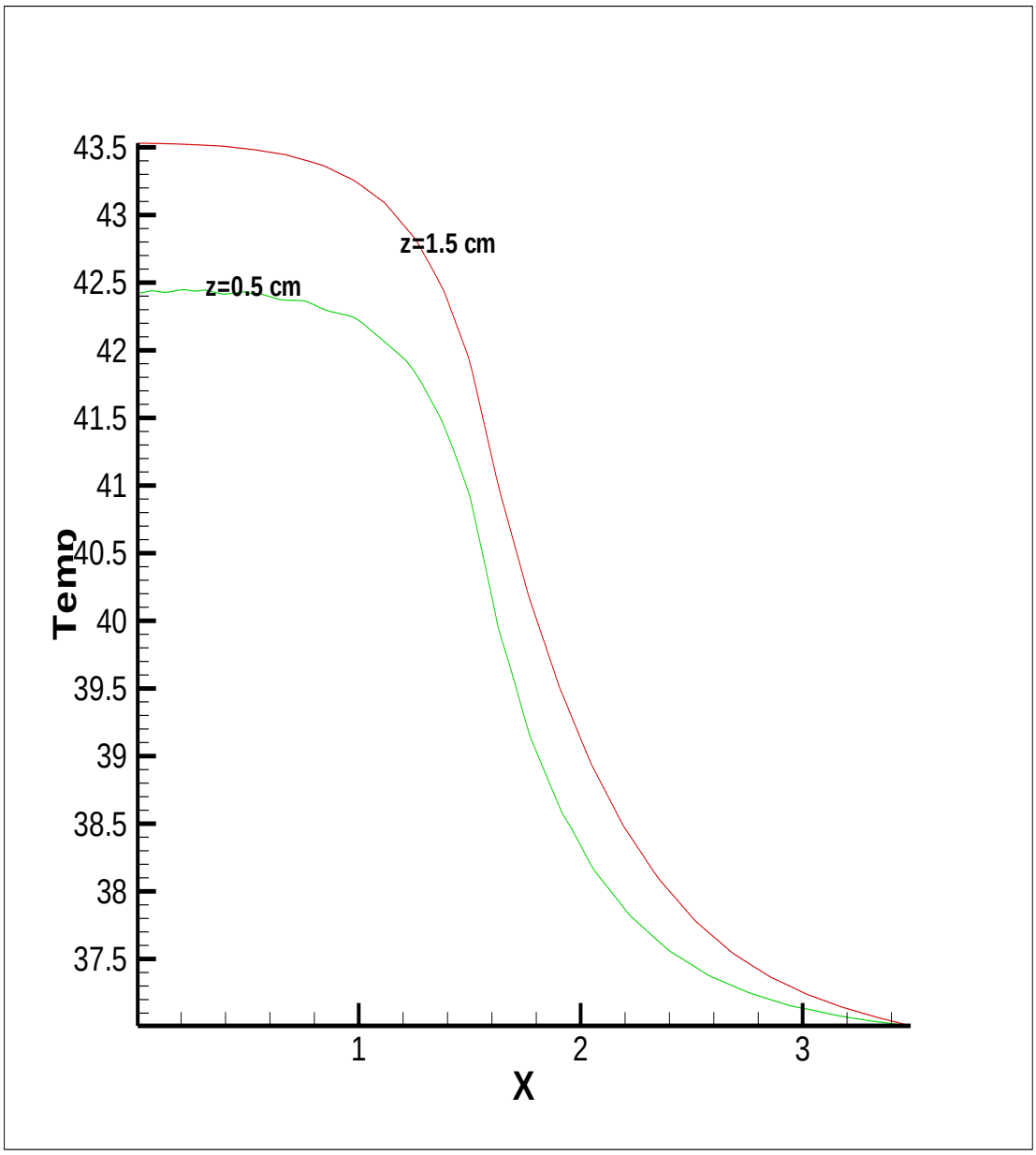

Figure 5.6: Variation of temperature w.r.t radius for the different heights

Because living tissue is complex, boundary condition can be either isothermal or fully adiabatic. If we continuously increase the height from 3 cm to to 200 cm, the temperature distribution is almost constant w.r.t heights as shown in figure 5.7 and 5.8, which removes the isothermal boundary condition at the edge of the tissue.

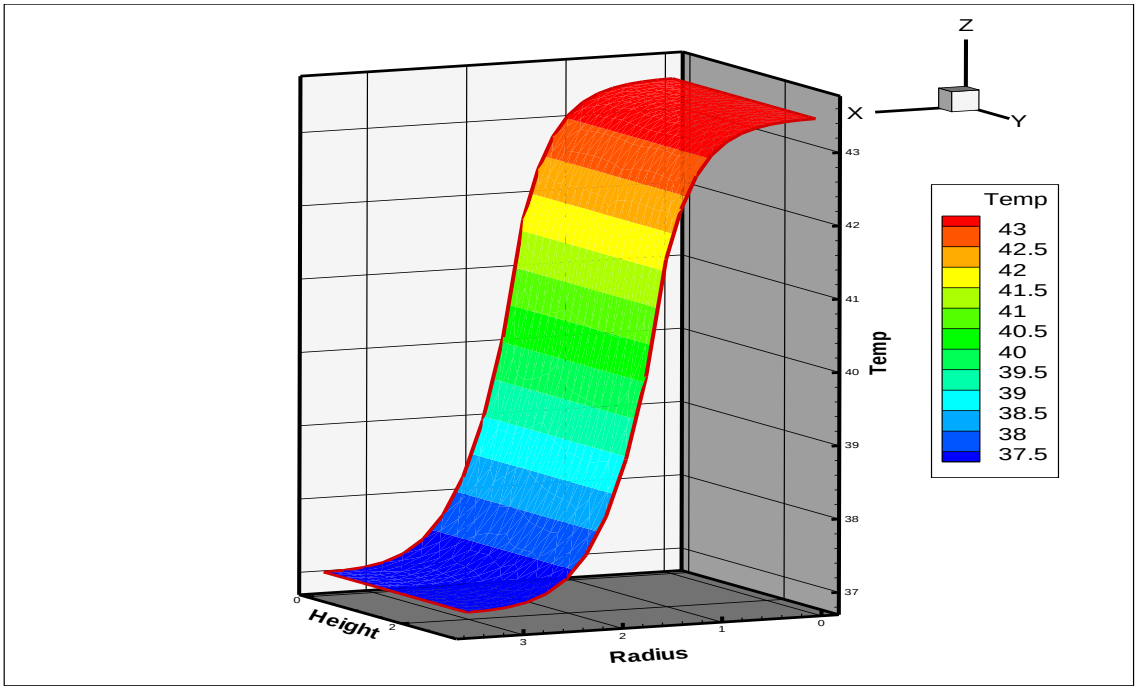

Figure 5.7: Temperature distribution in composite tissue for Adiabatic Boundary

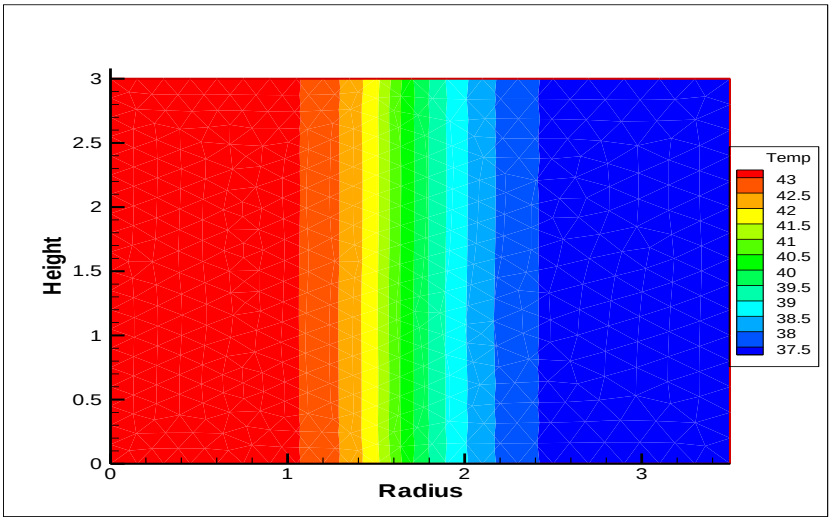

Figure 5.8: Contour profile in composite tissue for adiabatic boundary

From the figure 5.8, it is clear that temperature remains constant in z direction because of the adiabatic boundary condition so it is desirable to choose height as much as possible in order to choose adiabatic boundary condition which will eliminates the heat transfer in z direction.

5.4.3 Three Region Model

In this thesis, we are analyzing the temperature distribution in tumor and healthy tissue in hyperthermia cancer therapy. Temperature should be high enough to kill the cancer cell but same time it should cause minimum damage to the healthy tissue. In three region model, we divide the tumor region in to two regions and redistribute the nanoparticles such that only inner region has the particles and outer tumor region is free of nanoparticles. Thus we establish three region model to predict the steady state temperature distribution in tumor and surrounding normal tissue.

The three regions are defined in the figure: first region is ranging from 0 cm to 0.75 cm, second region is ranging from 0.75 cm to 1.5 cm and third region is ranging from 1.5 cm to 3.5 cm. The First and the second regions constitutes the tumor region while the third

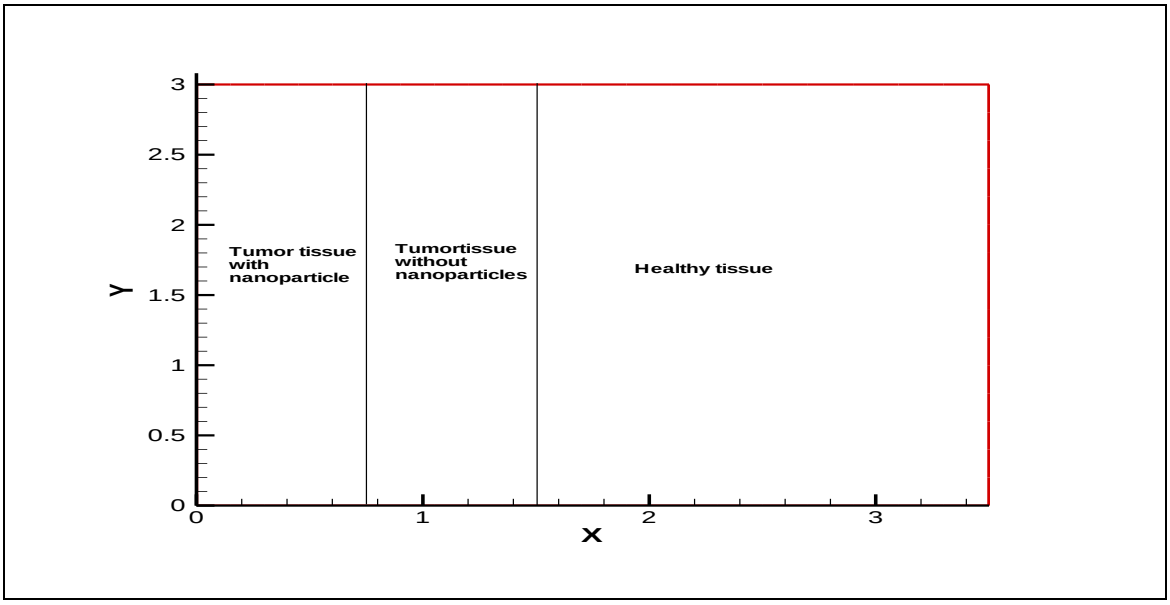

Figure 5.9: Three region model

region is the healthy region. Magnetic and thermal parameters will remain the same as we used for two region model.

Temperature contour for the composite tissue for three region model with nanoparticles present only in the centre part of the tumor region are displayed in figure 5.10.

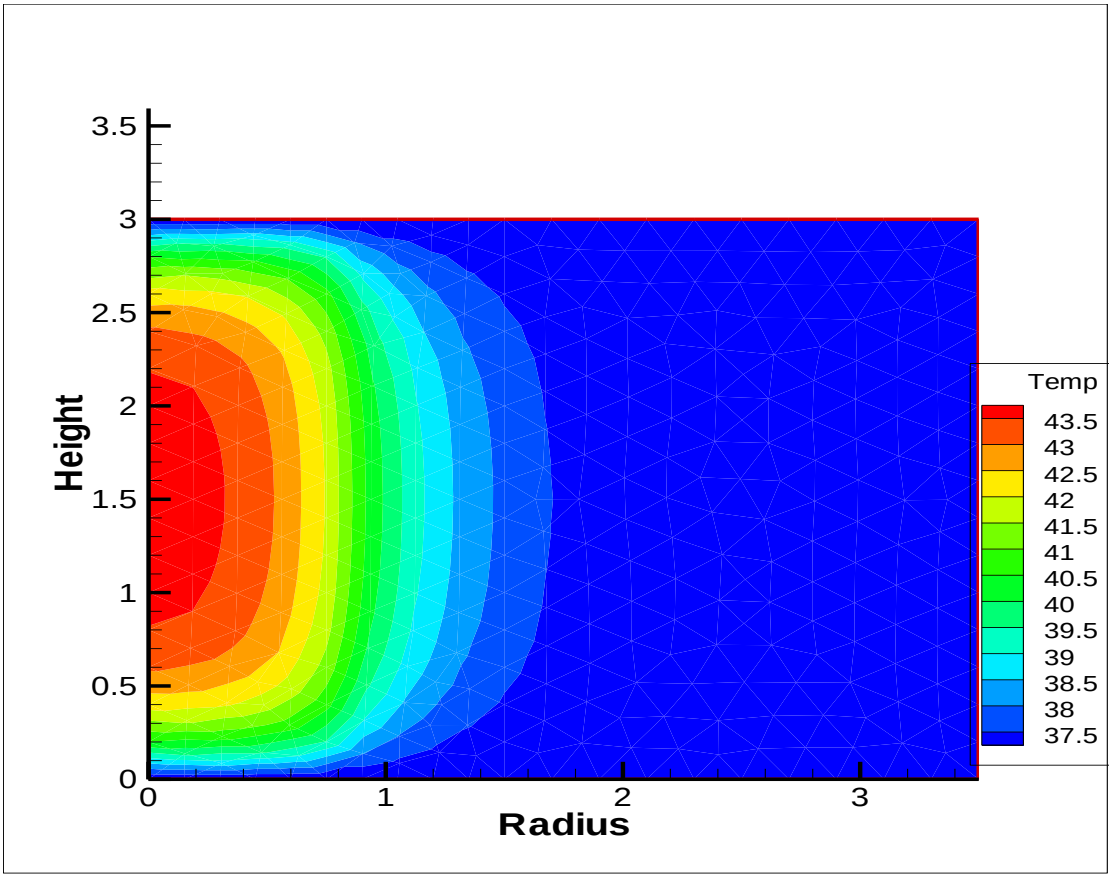

Figure 5.10: Temperature contour for three region model

It is clear that from the figure there is no significant difference in peak temperature in the centre of the tumor region compared with two region model.

Variation of the temperature with radius along a horizontal line at z = 1.5 cm is plotted in figure 5.11. Since the nanoparticles are present only in the centre region, the temperature lends in the healthy region are much lower with the maximum value below 38 ℃ therefore causing almost no overheating. Although absence of nanoparticles in the outer tumor region might be lower the therapeutic efficiency of the treatment to some extent.

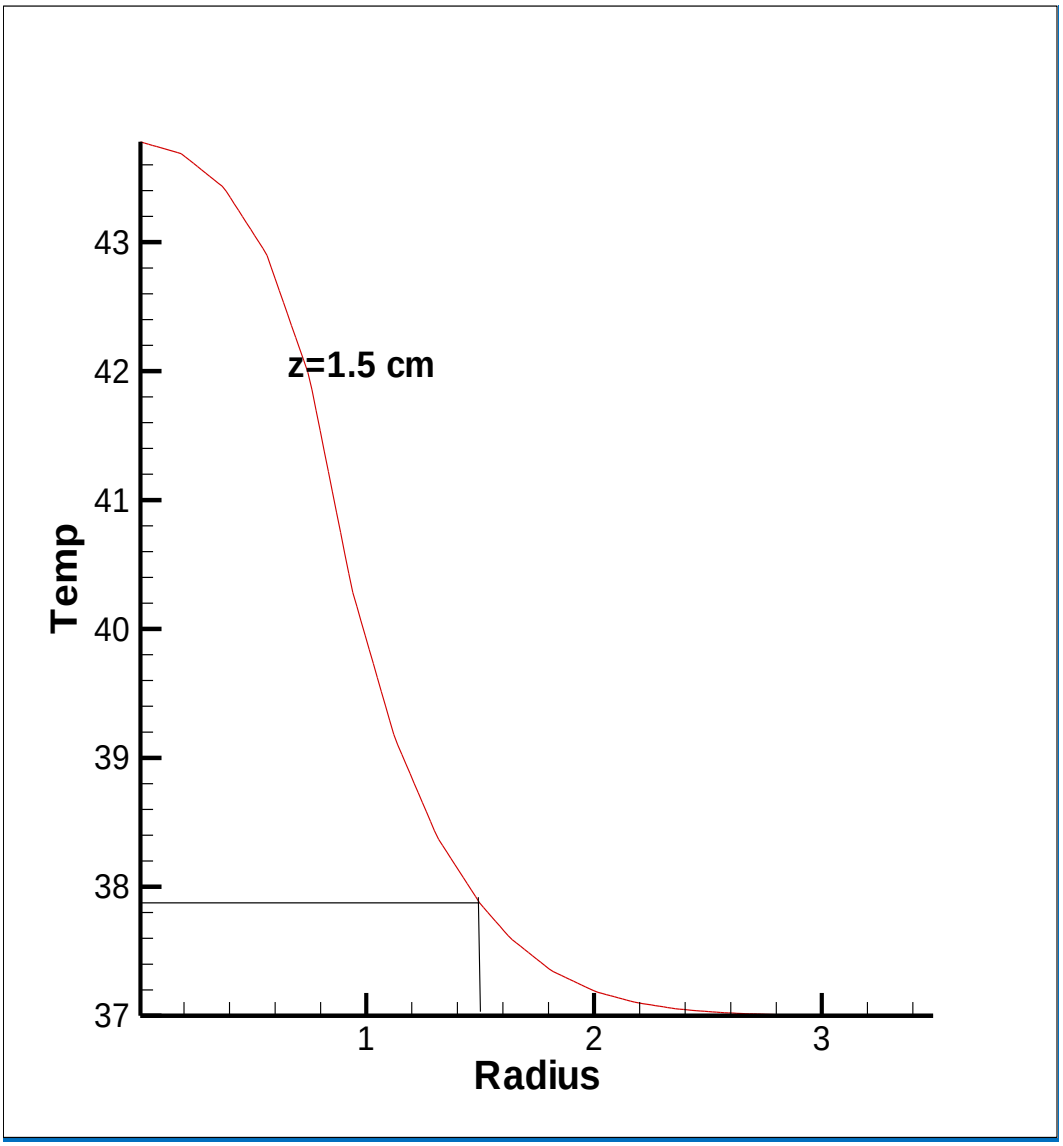

Figure 5.11: Radius Vs Temperature for three – region model for z=1.5 cm.

5.4.4 Effect of Blood Perfusion Rate

The effects of the blood perfusion through the tissue were investigated to determine their influence on the steady state temperature distribution when the nanoparticles were heated. Change in the blood perfusion rate gives the different temperature distribution. Variation of the temperature with radius ,at z = 1.5 cm for different blood perfusion rates presented in figure 5.12 below.

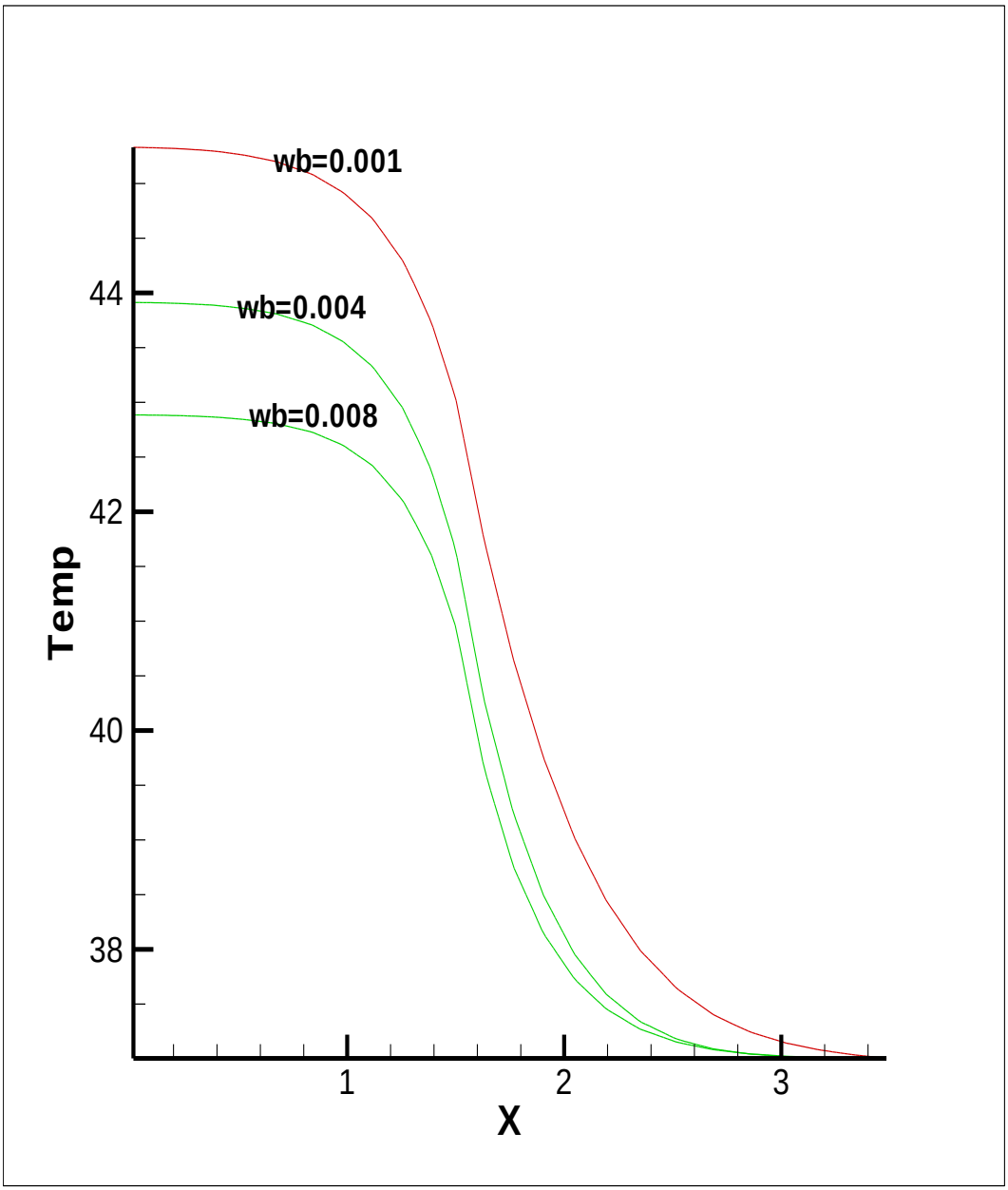

Figure 5.12: Steady state temperature distribution for the different blood perfusion rate for z=1.5cm for isothermal boundary condition.

The figure indicates that as the blood perfusion through the tissue increases, Steady state temperature levels decreases. Blood perfusion through the tissue created additional convection losses that lower the steady state temperature levels as the blood perfusion rate increased from 0.001 g cm^{-3} s^{-1} to 0.008 g cm^{-3} $s^{-1.}$

5.4.5 Hyperthermia Treatment for Irregular Domain

We discuss the temperature distribution for the composite tissue here that is easy to model but living tissues are complex. Tissue structure is quite heterogeneous in nature. Sometimes it is really necessary to find the critical temperature distribution for the given area. It is very difficult to find the temperature distribution for such irregular geometry or critical area with finite difference method. One of the advantages of the finite element method is that, it handles irregular mesh structure and irregular geometry that enables us to get the temperature distribution for the critical area.

5.4.3.1 Irregular Mesh Structure

Here we analyze the temperature distribution for the irregular mesh structure while keeping the size of the tissue and other parameters same as in the section 5.4.3. The irregular mesh for complex tissue is shown below in the figure 5.13.

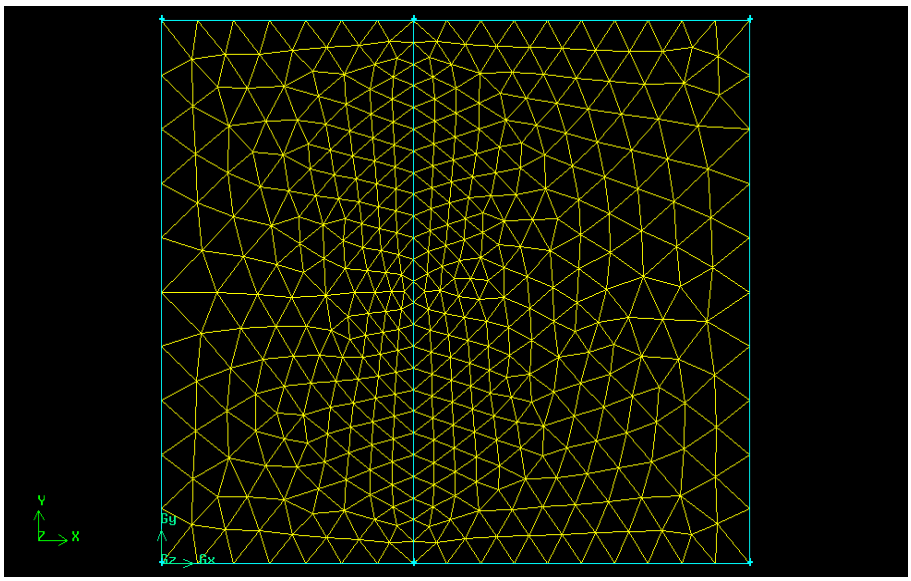

Figure 5.13: Irregular mesh structure for composite tissue model

Temperature distribution for the irregular mesh is displayed figure 5.14. If it is necessary to maintain the critical temperature for given area, finite element method gives smooth solution compared to finite difference method. In fact solution is not possible in the finite difference method for irregular mesh structure.

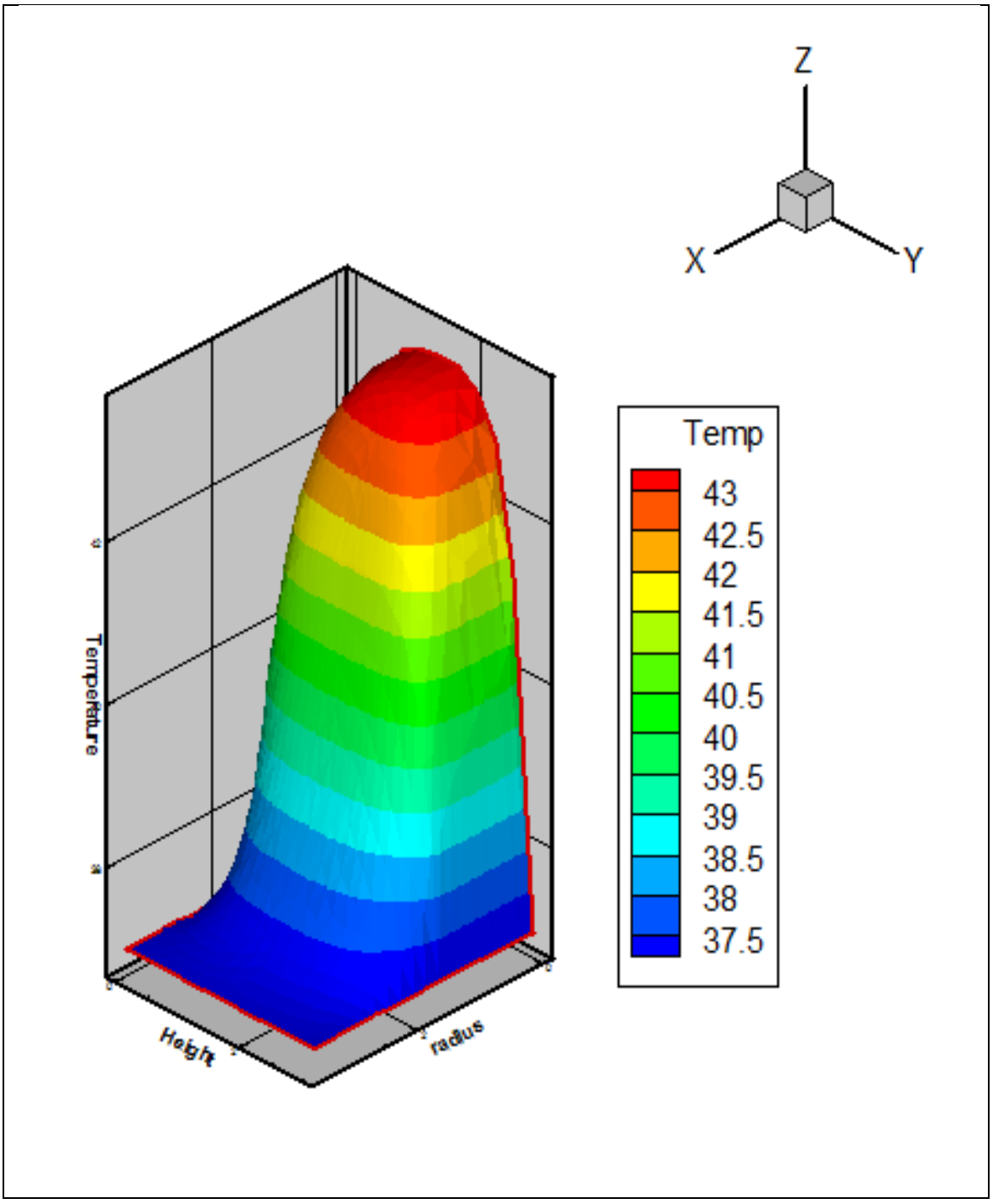

Figure 5.14: Temperature distribution for the irregular mesh structure

Contour plots for irregular mesh structure is shown in figure 5.15. Contours are similar to the once obtained for regular mesh case.

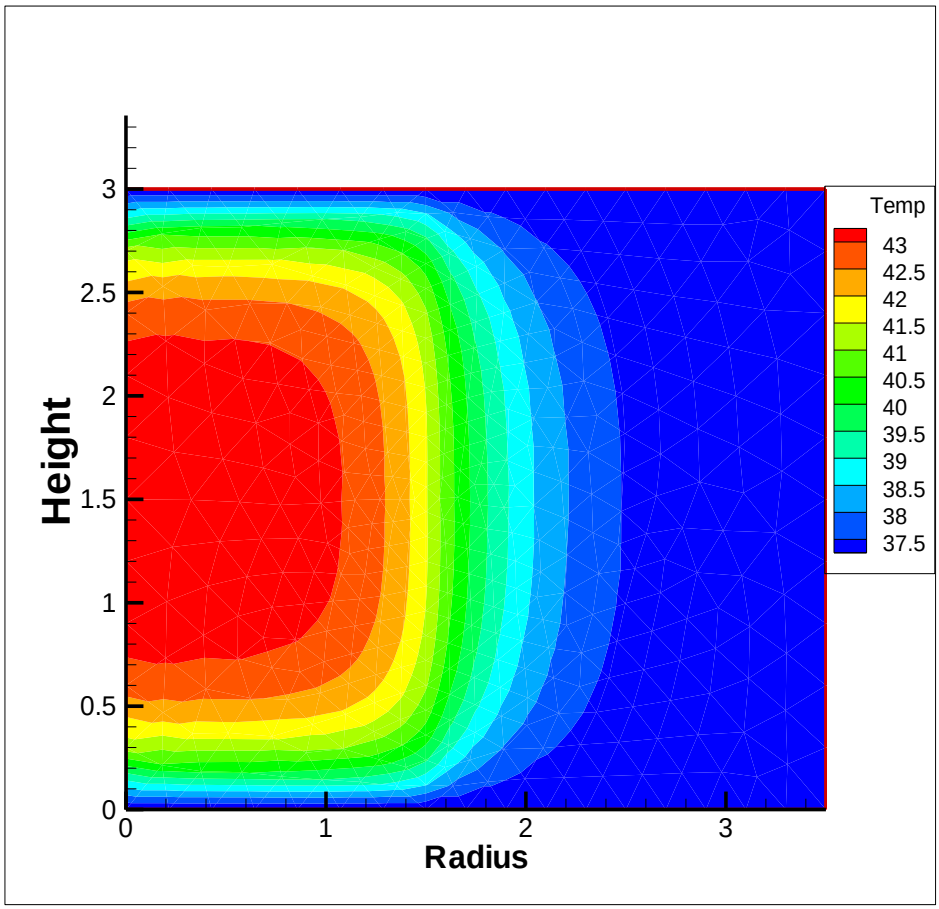

Figure 5.15: Temperature contour for irregular mesh

5.4.3.2 Irregular Geometry

As living tissue is very complex in the nature, sometimes it is necessary to do hyperthermia treatment for the irregular part of the body. An irregular geometry was considered underlining the ability of finite element method to handle irregular geometries and meshes. Two regions have been defined in the figure. Region A (red color) is tumor region and region B (blue color) is the healthy region. Thermal properties and all other parameters were considered to be the same as considered for regular geometry. Isothermal boundary condition was applied at the edge of the irregular geometry .Finite element solution for temperature field were obtained.

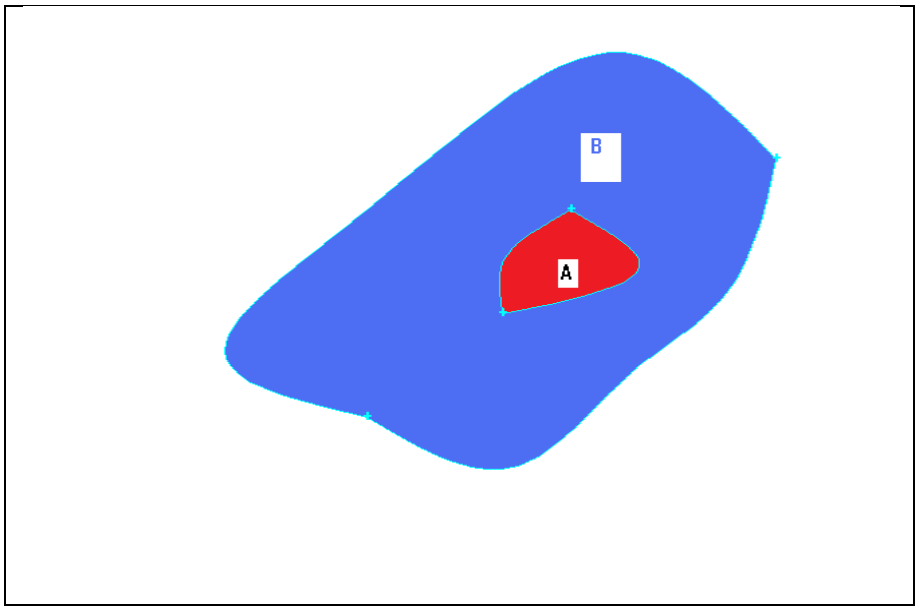

Figure 5.16: Irregular geometry model

Temperature distribution and temperature contours for the irregular geometry are displayed in figure 5.17 and 5.18 respectively.

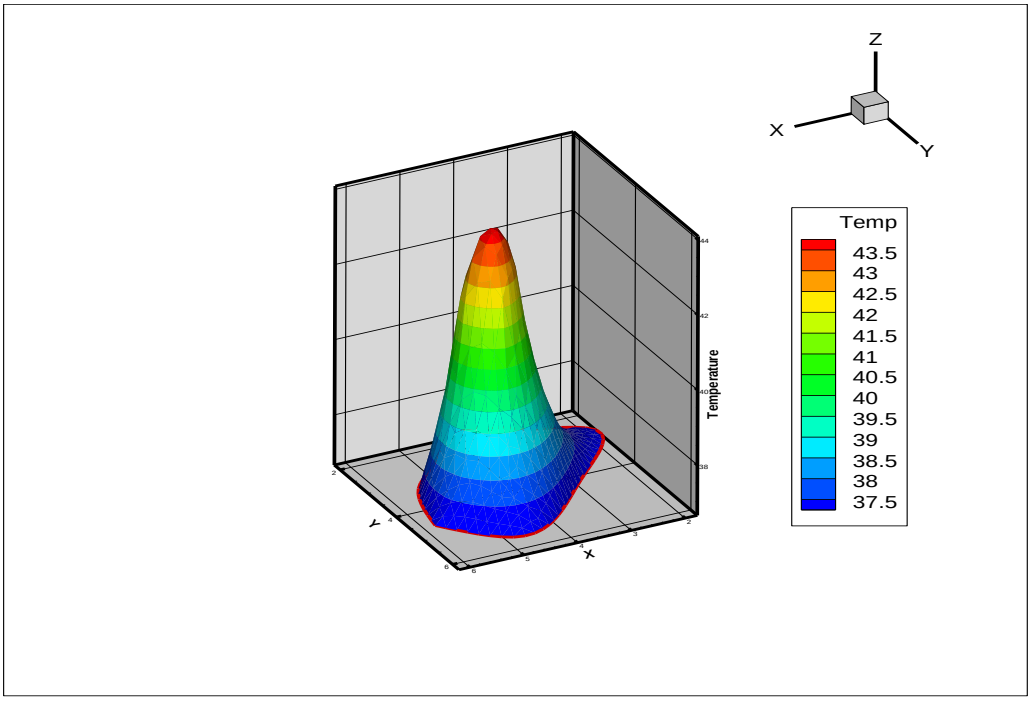

Figure 5.17: Temperature distribution for irregular geometry

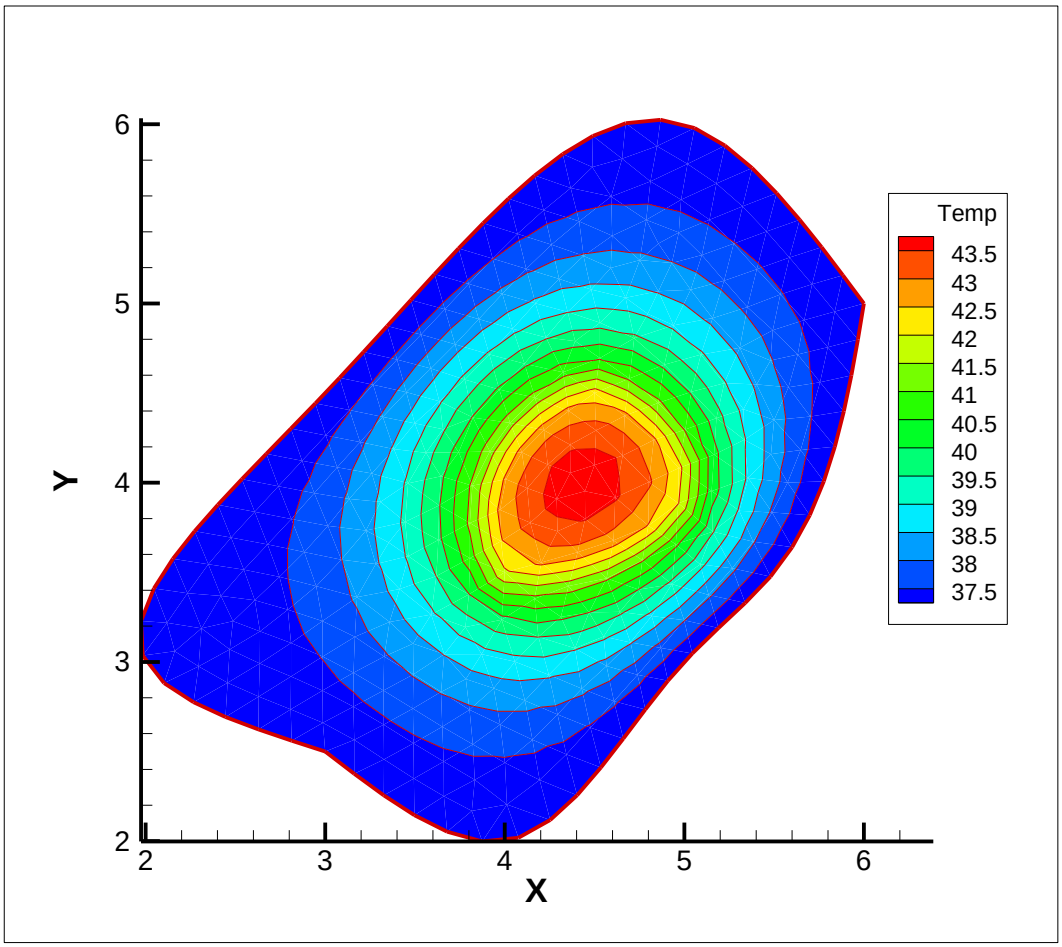

Figure 5.18: Temperature contour for irregular geometry

From the figures, it is clear that finite element method provides excellent temperature profile contours negotiating irregular geometries quite well.

CHAPTER 6

SUMMARY

This thesis presents the finite element analysis of bio-heat transfer in magnetic fluid hyperthermia applications on composite tissues. The thesis evaluating the temperature distribution by establishing multi-region bio heat equation using low Curie temperature nanoparticles dispersed in to the tumor tissue.

It has been shown that temperature in tumor region is around the 43℃ which is good enough to kill the cancer cell and in the healthy, it doesn't increase beyond 39℃ which will prevent damage to the healthy tissue. We have also shown that therapeutic effects depend on different factors like boundary conditions, blood perfusion rate and deposite pattern of the nanoparticles (three region model).

We considered isothermal and adiabatic boundary conditions and found that boundary conditions are less effective in temperature control. Analysis of different blood perfusion rate revealed that temperature levels in the tumor region decreases with increase in blood perfusion rate. Different distribution of nanoparticles also analyzed in order to optimize the localization of high temperature in the tumor region while minimizing the heating of the rest of the tissue. Also comparison between two region model and three region model was done and it was observed that with three region model there is better temperature control with no significant change in peak temperature in the tumor region. Two region model can keep all the tissue region at peak temperature which is good enough to kill the cancer cell in the tumor region but it would increase the overheating of the healthy region, which is undesirable.

Temperature distribution was also obtained for an example with irregular geometry and irregular mesh, which underlines the ability at FEM to negotiate irregular geometries and mesh structures, which is not possible with finite difference method as it can only be used for uniform

meshes. If hyperthermia cancer treatment has to be done for a critical irregular shape and sometimes if temperature control for some region is very critical then finite element method will give the better temperature distribution.

There is still lot of work to be done before achieving the accurate simulation of the temperature distribution especially with respect to the inhomogeneous localization of the magnetic nanoparticles and the complexity of the blood perfusion distribution within the tissue. Also the complex boundary condition in the real tissues and time dependent physiological parameters should be investigates in more detail.

REFERENCES

[1] Philips, J. L., *A Tropical Review of Magnetic Fluid Hyperthermia.* Retrieved from http://bama.ua.edu/~joshua/archive/aug05/Jennifer%20Phillips.pdf

[2] R. Xu, Y. Zhang, M. Ma, J. Xia, J. Liu, Q. Guo, and N. Gu, "Measurement of specific adsorption rate and thermal simulation for arterial embolization hyperthermia in the maghemite-gelled model," *IEEE Trans.Magn.*, vol. 43, pp. 1078–1085, 2007.

[3] Field, S.B.,and Bleehen,N.H.,"Hyperthermia in the Treatment Cancer,"*Cancer Treat Rev.,*vol.6,pp.63-69,1979.

[4] Rosenwieg RE. " Heating magnetic Fluid with alternating magnetic field*," j.Magn. Magn. Mater., vol.252,pp.370-374,2002*

[5] A. Jordan, R. Scholz, P. Wust, H. Schirra, T. Schiestel, H. Schmidt,and R. Felix, "Endocytosis of dextran and silan-coated magnetitenanoparticles and the effect of intracellular hyperthermia on humanmammary carcinoma cells in vitro," *J. Magn. Magn. Mater.*, vol. 194,pp. 185–196, 1999

[6] Strang, G**.**, & Fix, G. (2008).*An analysis of finite element method.* 2nd edn. Wellesley-Cambridge

[7] Byrom, T. G., Dewhirst, D. L., Huebner, K. H., & Smith, D. E. (2001). *The Finite Element Method for Engineers*. New York: Wiley-Interscience

[8] E. H.Wissler, "Mathematical Simulations of Human Thermal Behavior Using Whole Body Models," in *Heat Transfer in Medicine and Biology*, A. Shitzer and R. C. Eberhart, Eds. New York: Plenum Press, 1985, vol. 1, ch. 13, pp. 325–373.

[9] M..M.Chen and K.R.Holmes, "Microvascular Contributions in Tissue Heat Transfer," *Ann.NY Acad.Sci.*, vol.335,pp.137-150,1980

[10] S.Weinbaum and L.M.Jiji, "A New Simplified Bio-heat Equation for the effect of Blood

flow on Local Average Tissue Temperature," *J. Biomech. Engineering,*, vol. 114, pp.539-542, 1992

[11] Durkee JW, Antich PP, "Exact solution to the multi region time dependent bio heat equationwith transient heat source and boundary condition," *Phys.Med.Biol*.,Vol 36.,345-368,1991

[12] Durkee JW, Antich PP, "characterization of bioheat transport using an exact solution to the cylindrical geometry, multi region, time-dependent bio heat equation," *Phys. Med.Biol.,* vol, 36 pp. 1377-1406, 1991

[13] Durkee JW, Antich PP, Lee CE. "Exact solutions to the multiregion time –dependent bioheat equation 1: Solution development,"*Phys. Med. Biol.,*Vol.35, pp.847-867, 1990

[14] Durkee JW, Antich PP, Lee CE. "Exact Solution to the multiregion time-dependent bio heat equation II: Numerical evaluation of the solutions," *phys. Med Biol.,* vol.35, pp. 869-889, 1990

[15] Zhang, C., Johnson, D., & Brazel, C. (2009). Numerical Study on the Multi-Region Bio-Heat Equation to Model Magnetic Fluid Hyperthermia (MFH) Using Low Curie Temperature Nanoparticles. *NanoBioscience, IEEE Transactions on*, *7*(*4*), 267-275.

[16] Ozisik, M.N.,1993, Heat Conduction, 2nd ed., Wiley New York

[17] *Finite Element Method-Wikipedia,the free encyclopedia.* Retrived August 16, 2009 from http://en.wikipedia.org/wiki/Finite_element_method

[18] B. D. Cullity*, Introduction to Magnetic Materials*. Reading, MA: Addison- Wesley, 1972, pp. 91–105.

[19] http://cfdlab.uta.edu/~brian/research/head/validate.htm (Accessed: 17 July 2009).

[20] Bagaria, H., & Johnson, D. (2005). Transient solution to the bioheat equation and optimization for magnetic fluid hyperthermia treatment. *International Journal of Hyperthermia*, *21*(*1*), 57-75.

[21] Q. A. Pankhurst, J. Connolly, S. K. Jones, and J. Dobson, “Application of Magneticnanoparticles in biomedicine,” *J. Phys. D: Appl. Phys.*, vol.36, pp. R167–R187.

BIOGRAPHICAL INFORMATION

Kamalkumar N Chauhan was born in Surat, India in 1985. He received his bachelor of engineering in Mechanical Engineering from Sardar Patel University. After completing his bachelor degree, he worked as Engineering Trainee in the Essar Steel Ltd, Hazira, India. He joined University of Texas at Arlington to pursue his graduate studies in Mechanical Engineering. His area of inerest includes Finite Element Method and CFD.